

REPORT NO. E2012:06

Climate Sensors in Trucks  
– Master Thesis at Volvo Group

Åsa Leander  
Marika Turesson

Supervisor: Ph.D. student Mattias Gruber

Examiner: Professor Jan-Olof Dalenbäck

Department of Energy and Environment  
*Division of Building Services Engineering*  
CHALMERS UNIVERSITY OF TECHNOLOGY  
Gothenburg, Sweden, 2012

**Climate Sensors in Trucks  
– Master Thesis at Volvo Group**

**ÅSA LEANDER  
MARIKA TURESSON**

**© ÅSA LEANDER & MARIKA TURESSON, 2012.**

**Technical report NO. E2012:06  
Department of Energy and Environment  
CHALMERS UNIVERSITY OF TECHNOLOGY  
SE-412 96 Gothenburg  
Sweden  
Telephone +46 (0)31 772 1000**

**Print service  
Gothenburg, Sweden 2012**

# **Abstract**

Good air quality and temperature is not only pleasant but also a health issue and since the cabin of a truck is a work environment, the same demands as in other working spaces should be met. Volvo Group is a company which has the will of continuously improving their technology and has a strong safety culture, therefore the climate in the cabin is hence considered an important issue. There are four truck brands within the Volvo Group: Volvo Trucks, Mack Trucks, Renault Trucks and UD Trucks. The intention is that this thesis can contribute with knowledge to all the truck brands within the Volvo Group.

To control the climate inside the cabin of a truck several sensors can be used. This master thesis aims at increasing the knowledge, mainly concerning a possible future solar sensor. A solar sensor in combination with a Climate Control Unit (CCU) can be used to forecast an increase in temperature in the cabin and to compensate for the thermal discomfort felt by a person situated in sunlight. The thesis started with a simulation of the heat balance of the truck in order to find the required accuracy and time constant of the solar sensor. Tests were performed to evaluate how a solar sensor would be affected by the windshield and finally a benchmark of the solar sensor was performed.

The simulations show that the time constant of a solar sensor should be shorter than two seconds and that the accuracy should be within  $\pm 6$  W. There are several manufacturers of solar sensors with shorter time constants than required, however the accuracy of solar sensors is difficult compare between the manufacturers. The design of the sensors and their casing has a great impact on the performance of the sensor, as well as the placement of the sensor and the materials in the near surrounding. It is difficult to predict exactly how a specific sensor will perform in a particular application, hence physical tests will be needed to get exact results.

# Sammanfattning

Bra luftkvalitet och klimat är inte bara en fråga om trivsel utan även en hälsofråga. Eftersom lastbilshytten är en arbetsplats så bör samma krav sättas på luftkvaliteten där som på andra arbetsplatser. AB Volvo är ett företag med viljan att ständigt förbättra tekniken i deras produkter och de har en stark säkerhetskultur, därför anses klimatet i kabinen vara en viktig fråga. Det finns fyra lastbilsärken inom AB Volvo; Volvo Trucks, Mack Trucks, Renault Trucks och UD Trucks. Examensarbetet avser att bidra med kunskap som kan användas vid utveckling av klimatstyrning i alla lastbilar inom AB Volvo.

För att styra klimatet i hytten används ofta en uppsättning av sensorer. Examensarbetets intention är att öka kunskapen kring framför allt de så kallade solsensorerna. En solsensor tillsammans med klimatregleringssystemet kan användas för att förutspå en temperaturökning i kabinen och för att kompensera för den upplevda temperaturökningen när en person träffas av solljuset. Examensarbetet startade med att simulera värmebalansen i hytten för att ta fram krav på noggrannhet och tidskonstant för en möjlig framtida solsensor. Tester gjordes för att ta reda på hur solsensorer fungerar i kombination med en vindruta och slutligen gjordes även en marknadsundersökning för att se vilka solsensorer som finns på marknaden.

Simuleringarna visar att solsensors tidskonstant bör vara kortare än två sekunder och att noggrannheten bör vara inom  $\pm 6$  W. Det finns flera tillverkare av solsensorer som uppfyller tidskravet men noggranheten är ändå svårare att jämföra mellan sensortillverkare. Solsensors konstruktion och hölje har stor inverkan på sensorns funktion, det har även placeringen av sensorn och matrialen kring där sensorn skall placeras. Det är komplicerat att förutspå exakt hur en specifik sensor kommer prestera i en särskild tillämpning och miljö, därför är test nödvändiga för att få exakta resultat.

## **Abbreviations**

AQS	Air Quality Sensor
CAD	Computer Aided Design
CCS	Climate Control System
CCU	Climate Control Unit
GTT	Global Trucks Technology
NTC	Negative Temperature Coefficient
OAT	Outdoor Air Temperature
VOC	Volatile Organic Compound

## Preface

The master thesis has been performed at Volvo Group within the division Global Trucks Technology. Tests were performed at the sensor manufacturer Accel in Lithuania, and simulations were performed at the Division of Building Services Engineering at Chalmers University of Technology. The aim of the study was to increasing the knowledge, mainly concerning a so called solar sensor which can be used to control the climate in the truck cabin.

We would like to express our gratitude to Henrik Fellbom, Björn Mårdberg, Joachim Osbeck, Paul Petersson and other personnel at AB Volvo. We would also like to thank Magnus Nilsson, Arvydas Maldžiūnas and the employees at Accel. Finally we would like to thank Mattias Gruber for all the help and support during the simulations and the rest of the thesis work.

# Contents

Abstract	iii
Sammanfattning	iv
Abbreviations	v
Preface	vi
Contents	vii
1 Introduction	1
1.1 Scope	1
1.2 Method	1
2 Background	3
2.1 Sensor Technology	3
2.2 Sensors Used to Control the Climate in Vehicles	6
2.3 The Climate Control System	7
3 Sun Angles Influence Sensor Performance	9
4 Simulation of the Heat Balance	13
4.1 Assumptions	13
4.2 Accuracy	14
4.3 Time Constant	18
4.4 Summary, Simulation	21
5 Benchmark	23
5.1 Method	23
5.2 Benchmark of Solar Sensor	24
6 Test of Solar Sensors Developed by Accel	29
6.1 Equipment	29
6.2 Source of Error	31
6.3 Tests Performed	32
6.4 Conclusions	45
7 Ideas for Improvements Outside the Scope	47
7.1 CO <sub>2</sub> Measurement	47
7.2 How to guarantee good air quality	47
7.3 Maximum Ventilation Button	48
8 Results - Summary	49
9 Discussion	51
9.1 Time Constraints and Accuracy	51

9.2	Benchmark	52
9.3	Placement	53
9.4	The Tests	53
10	Recommendations	55
	Works Cited	57
	Figure Sources	58
	Appendix A – Resistance Sensor, Wheatstone Bridge and Transfer Function.	59
	Appendix B – Sensor Parameters	61
	Appendix C – Some Basic Types of Sensors	65
	Appendix D – Verification of the Model	71
	Appendix E – In Data, Simulations	73
	Appendix F – Cooling Potential	75
	Appendix G – Outside Sun Load	77
	Appendix H – Benchmark of AQS and Fog Sensor	79
	Appendix I – Equations Used in Simulink Model	81

# 1 Introduction

This master thesis was performed within the division Global Trucks Technology (GTT) at the Volvo Group. GTT is developing the technology used in the different truck brands within the Volvo Group, namely Volvo Trucks, Renault Trucks, Mack Trucks and UD Trucks. The Volvo Group is continuously improving their products and the thesis is focusing on the possibilities of improving the climate control in the cabin.

High demands are set on the comfort in work places. A big part of this comfort is dependent on the air quality and the air temperature. Good air quality and a comfortable temperature do not only provide a pleasant environment for the driver but is also a health and safety issue. There are several ways of controlling the climate in the cabin of a truck and new ideas are constantly evolving. An important part of the automatic climate control is the sensors used to gather the necessary information from the controlled system.

Important parameters that can be measured are the amount of unhealthy substances in the air, the air temperature and the risk of mist formation on the windshield. These measurements can be performed in several ways. In this thesis the idea is that the climate in the cabin can mainly be controlled by four sensors. An *Air Quality Sensor* – measuring the amount of unhealthy gases in the air, a *Temperature Sensor* – sensing the temperature in the cabin, a *Fog Sensor* – forecasting the risk of misting on the windshield and a *Solar Sensor* – measuring the heat influx through the windows of the truck. Early on in the thesis it was understood that a solar sensor can be of high importance when controlling a climate system. Hence the thesis was focused on the solar sensor.

## 1.1 Scope

The assignment given by Volvo for the thesis was to look into sensors that can be used to control the climate inside the cabin and to update this knowledge within the Volvo Group. The objective chosen was to identify how fast and accurate a solar sensor would have to be, to examine which solar sensors that are present on the market and to investigate how a solar sensor should be positioned in a truck. It was also of interest to examine how the performance of a solar sensor is affected by a windshield glass used for the trucks within the Volvo Group.

## 1.2 Method

In order to fulfill the chosen scope the methodology of the thesis was divided into the following five main categories:

- A literature study, to gather all background information needed.
- Simulation of the heat balance of a truck, to get the required accuracy and time constant for a solar sensor.
- Investigate the impact of the placement of a solar sensor by calculations and tests.
- Perform a benchmark of solar sensors, Fog sensors and AQS sensors.
- Perform physical tests on solar sensors.

### **1.2.1 Literature Study**

The literature study was performed to gather knowledge about the technological aspects of different types of sensors used in the climate system, about their connection with the climate control system and about the air handling system of a vehicle. The literature revised were books regarding the field of sensor technology and climate control in vehicles, other literature studied was technical reports provided by both Volvo and several sensor manufacturers.

### **1.2.2 Simulation of the Heat Balance**

To simulate the heat balance of the truck a model in Simulink was used. This model was developed by the Ph. D student Mattias Gruber at the institution of Building Services Engineering at Chalmers University of Technology. (Gruber, 2012) The model was originally developed for simulations of the heat balance of buildings but with some modifications the model was used to simulate the heat balance of a truck, these modifications are further explained in chapter 6. The aim of the simulations was to find the required accuracy and time constant of a solar sensor.

### **1.2.3 Placement of Solar sensor**

The impact of the placement of a sensor was investigated by calculations and by physical tests. A common placement of the solar sensor in other vehicles is in the middle of the dashboard near the windshield. For this placement of the sensor the impact of different elevation angles of the sun was evaluated and tested.

### **1.2.4 Benchmark**

The benchmark started with a search of suitable manufacturers, this search was performed by gathering available information at Volvo Group and by searching on the internet. The suppliers found were then contacted and asked to provide the information available about their sensors. The information provided by the manufacturers was evaluated and the functional parameters of the sensors were compared.

### **1.2.5 Test of Solar Sensors**

Several tests were performed in cooperation with the sensor manufacturer Accel situated in Lithuania. The equipment and the know-how of the test procedures were provided by Accel.

In the tests, two light sources were used, one from Ocean Optics and a Solar simulator from Newport. In addition a spectrometer and fiber optic wires by Ocean Optics were used together with two voltmeters. More information concerning the equipment is found in chapter 8.

A windshield, used by one of the truck manufacturers within the Volvo Group, was used in the tests at Accel to evaluate its impact on the performance of a solar sensor. In addition, the impact of different casings of the sensors was tested, Accel provided their infrared casing and their casing with a dimming function. Finally it was tested whether the results from the physical tests differs from calculated results from data provided by manufacturers.

## 2 Background

This chapter aims at providing the reader with the background information needed to understand the basic principles of sensors and the basic functions of the air handling system in vehicles.

### 2.1 Sensor Technology

A sensor is a device used to convert a physical phenomenon to an electrical signal, hence a sensor can be seen as the interface between the physical world and a computer. (Wilson, 2005) Another part of the electrical system is the transducer which is a device that converts energy to another form, but not to an electrical signal, hence a sensor can be preceded by several transducers in the sensing system. The actuator is also a part of the control system and it converts an electrical stimulus to a non-electrical signal, which is the opposite function of that of the sensor. (Fraden, 2004)

#### *Feedforward and feedback control*

Sensors can be used in feedforward loops or in feedback loops. Feedforward is when the signal from a sensor is used to forecast a change or sense a disturbance, for instance an increased sun load which can result in a temperature increase. Then the control system can prevent the temperature from increasing before happening. Feedback control is used to control so that the actual parameter sensed, for example temperature, is within limits. If there is an error between the temperature that it should be and the actual temperature, then the error is eliminated by the control system and the actuators. (TECHMATION)

#### 2.1.1 Physical Principles of Sensing

The physical principles of a sensor are those principles that allow the sensor to sense its surrounding. An example of this is the expansion of a material due to heat and as a result the voltage over the material changes. This change in voltage can be measured and a certain change in voltage can be accredited a certain change in the physical property that gives rise to the expansion of the material. (Fraden, 2004)

In order to transform a physical property into an electrical signal a resistor, a capacitor or an inductor can be used. Since it is the electrical characteristics and the output signal from the sensor that influence the performance of the circuit, therefore a successful application of a sensor depends on a correct choice of physical property on which the sensor is based on. (Wilson, 2005)

#### *Resistor*

A *resistor* is a passive element that acts as a obstacle to the current in an electric circuit. The *resistance* of a material is determined by Ohm's law according to equation 1.

$$R = \frac{V}{i} \quad (1)$$

Where R is the resistance, V is the voltage and i is the current. (Fraden, 2004)

The basic design of a resistive sensor consists of two resistors. One of the resistors is called the sense resistor and its properties vary with for example the temperature, the other resistor is called the load or the reference resistor. The load resistor must have a larger resistivity than the sense resistor to be able to determine if the current is close to constant and to assure that the circuit offers a good linearity. Good linearity is sought because then the deviation from a linear transfer function is as small as possible. One method to measure the resistance of a resistive sensor is by applying a voltage source to force a current to flow through the circuit. A basic setup for a resistive sensor called a voltage divider is shown in figure 1. (Wilson, 2005)

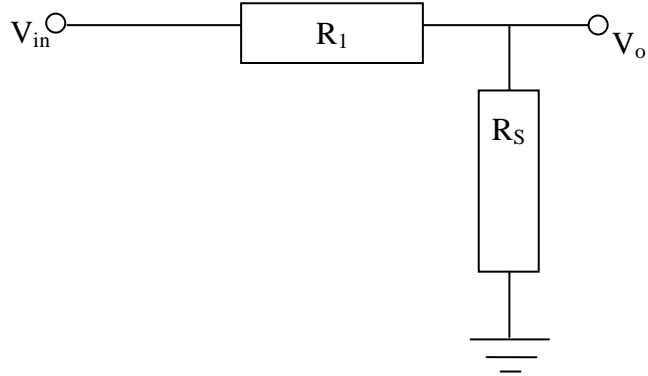


**Figure 1.**  $R_s$  is the sensing resistance and  $R_1$  the load resistance.

Further information can be found in appendix A.

### Capacitor

A *capacitor* consists of two electric conductors separated by a dielectrical element, often called insulator. The *capacitance C* of a capacitor depends on the relative position, the shape of and the medium in between the plates that constitutes the capacitor. The simplest type of a capacitor is two parallel plates separated by a type of insulator. The current changes with the capacitance according to equation 2.

$$i = C \frac{dV}{dt} \quad (2)$$

Where  $i$  is the current,  $C$  is the capacitance and  $V$  is the voltage. (Alciatore, o.a., 2007)

A high quality capacitor is a capacitor for which both the structure and the relative distance are stable, its properties should not vary with for example temperature or pressure. However, when a capacitor is used as a component in a sensor the purpose of it is to vary with the changes in the close environments. Hence a not so high quality capacitor is to be used. (Fraden, 2004) An example of a capacitive sensor is the capacitive relative humidity sensor. The dielectric constant changes when the relative humidity of the air changes, this result in a change of the capacitance and this is what can be measured. A simple capacitive sensor can have the same setup as the voltage divider shown in figure 1 above. Either a capacitor or a resistor can be used as the load resistance. (Wilson, 2005)

### *Inductor*

An *inductor* is a passive element in an electric circuit that stores energy in its magnetic field. The inductor is often wound in loops in order to increase the magnetic field. The *inductance* of an inductor can be calculated from its geometrical factors such as number of windings of the coil and size. The voltage changes with the inductance as stated in equation 3.

$$V = L \frac{di}{dt} \quad (3)$$

Where V is the voltage, L is the inductance and i is the current. (Fraden, 2004)

The simplest type of an inductor is a wire coil. (Alciatore, o.a., 2007) Just as the resistor and the capacitor the inductor is a resistive element, hence the voltage drop over the inductor can be compared with the voltage drop over another passive element in a divider circuit. However, the inductors are often more expensive to produce and therefore they are not as common as the resistive sensors using a resistor. The inductor can be combined with for example a resistor to form a voltage divider. (Wilson, 2005)

## **2.1.2 Sensor parameters**

There are several parameters or constants defining the performance of a sensor. In this thesis focus has been on two of them, the accuracy and the time constant. More parameters are found in appendix B.

### *Accuracy*

*Accuracy*, or sometimes referred to as *inaccuracy*, is often defined as the maximum error between actual and ideal output signal. (Wilson, 2005) The inaccuracy can be computed from the difference between the value that is computed from the output voltage and the input stimuli. (Fraden, 2004)

The accuracy is in most cases used to determine the worst case scenario performance of the sensor. (Fraden, 2004)

### *Rise time and time constant*

The rise time and time constants are parameters used to quantify how quickly a sensor or a control system reacts. The time constant is the time it takes for the sensor to measure 63 % of the final value and the rise time is the time it takes for the sensor to measure 90 % of the final value. It is unusual to measure the time it takes for the sensor to reach its final value due to sometimes long lasting oscillations, which is shown in figure 2. (Lennartson, 2002)

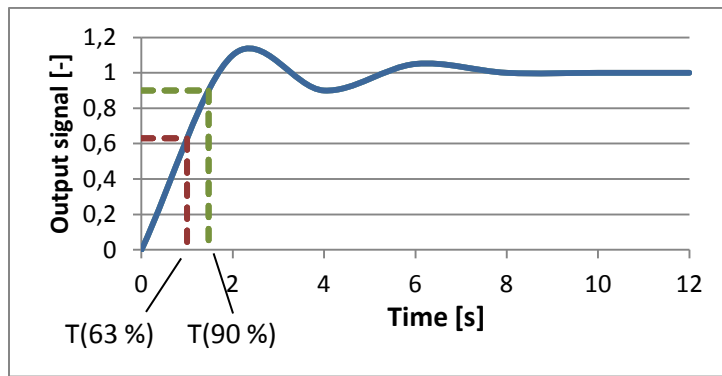


**Figure 2.**  $T(63\%)$  represent the time constant and  $T(90\%)$  represent the rise time.

## 2.2 Sensors Used to Control the Climate in Vehicles

This study is focused on three of the sensors that can be used to control the climate system in a truck; one sensor measuring the solar intensity influence from the sun, one measuring the risk of mist occurring on the windshield and one measuring the quality of the air at the intake. (Fellbom, 2012) For more information and some more types of sensors see appendix C.

### 2.2.1 The Solar Sensor

The solar sensors used by several vehicle manufacturers today measures the angle of the sun and the sun load. (Volvo GTT, 3) The sensor often consists of two photodiodes which constitute the sensing elements. (Mårdberg, 2012) The two sensing elements are often placed with an angle between them, one slightly to the left and one slightly to the right. (Volvo GTT, 3) This in order to detect on which side the sun beams hit the cabin and to cool this side with for example increased amount of supply air. (Fellbom, 2012)

The sun load is measured to be able to foresee and prevent an increase in temperature and to compensate for the increased temperature felt by a person situated in sunlight, by using a feed forward control system. (Mårdberg, 2012)

### 2.2.2 The Air Quality Sensor

The Air Quality Sensor (AQS) is designed to be placed in the air inlet of vehicles. The AQS can measure increases in CO and NO<sub>2</sub> levels. (Volvo GTT, 3) The basic idea with the sensor is to send a signal to the climate control module when an increase in CO, NO<sub>2</sub> or other oxidizing or reducing gases, occurs. The signal would then be used together with signals from other sensors and can result in closure of the flap that controls the fresh air inlet, when the flap is closed all air is recirculated. (Mårdberg, 2012) The sensor could be adaptive, meaning that if the surrounding air is rather clean from polluting gases it would react on small increases and if the surrounding air contains a relatively high level of polluting gases it would only react when the gas concentration increases even more. (Mårdberg, 2012)

The air can also be filtered with an active carbon filter that reduces the amount of the CO and NO<sub>x</sub> entering the cabin, however the filter would not be 100 % effective and that is why the air in situations with high levels of polluting gases is recirculated. (Fellbom, 2012)

### **2.2.3 Fog sensor**

The fog sensor used in vehicles often contains one relative humidity sensor combined with a sensing element sensing the temperature of the windsheeld and one NTC-thermistor measuring the temperature of the cabin air. (Volvo GTT, 3) The humidity sensor is often a capacitive sensor and the capacitance of the capacitor varies with the humidity since the dielectric element in most cases is a polymer which absorbs or releases water proportional to the surrounding air humidity. (Volvo GTT, 3)

The dewpoint can be calculated from the relative humidity and the cabin air temperature. The dewpoint would then be compared with the temperature of the windshield. If the temperature of the windshield is lower than the calculated dewpoint misting can occur. If there is a risk of mist formation on the windshield the supply air leaving the defrost nozzles can be heated. Another possibility is to place the sensor directley on the windshield and when the relative humidity is exceeding a certain level the sensor can send a signal to the climate control system that misting can occur, without calculating the dew point. The system can be tuned in during tests and the signal would depend also on the outside temperature. (Fellbom, 2012)

### **2.2.4 The Sensors and the Control System**

If there is a risk of mist occurring on the windshield a fog sensor would sense this and send a signal to the control system. The signal from the fog sensor should always be prioritized since mist formation on the windshield is a safety issue. The second most important signal could be the one from the solar sensor, this is due to that with this signal it is possible to forecast an increased temperature in the cabin and to prevent it before happening. Both the fog sensor and the solar sensor signals are used as feedforward signals in the control system.

There is also a temperature sensor checking if the temperature is right in the cabin, this signal is used as feedback control. The signal from the solar sensor is sometimes considered more important than the temperature sensors signal because of that the temperature sensor reacts much slower than the solar sensor due to inertia of the air in the cabin.

## **2.3 The Climate Control System**

The Climate Control System (CCS) in a truck controls the heating and cooling of the incoming air, the incoming air volume and whether outside air or recirculated air shall be used. With the help of ducts and dampers the CCS can be used both to provide a comfortable cabin climate and as a defroster to remove frost occurring on the windshield. (Daly, 2006) In figure 3 a schematic picture of CCS is shown.

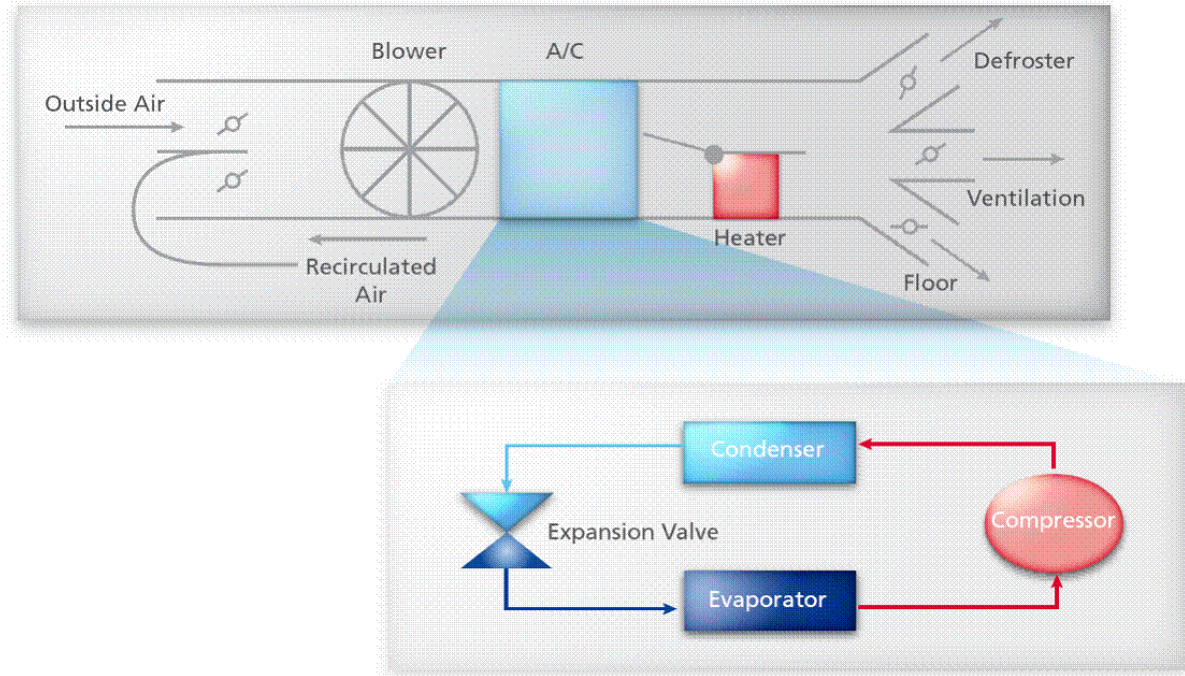


**Figure 3.** Schematic picture of the CCS and a close up of the AC system.

The CCS contains ducts, a blower, an Air Conditioning (AC) system, a heater and several valves. As seen in the figure, it is possible to recirculate air from the cabin, this is done to save energy hence cooling and heating demand is lowered. The AC system itself consists of four components; a compressor, a condenser, an expansion valve and an evaporator. The compressor compresses the superheated refrigerant vapor, during the compression the pressure and temperature of the vapor increases rapidly. After the compressor the vapor enters the condenser where rejects the heat and return to the liquid state. The condenser works as a heat exchanger and is situated in the front of the truck where the airflow is high. When the refrigerant leaves the condenser it is a liquid. The next part in the system is the expansion valve. The functions of the valve are; separate the high pressure side from the low pressure side and to meter the amount of refrigerant that is circulating and by that measure the cooling capacity. After the expansion valve the refrigerant enters the evaporator where it absorbs the heat from the cabin air. (Daly, 2006) After the AC system the air got the right temperature and can be distributed into the cabin.

The AQS, fog and solar sensors that are studied in this thesis can be used to facilitate the control of the climate in the cabin, they provide the CCS with information about the current status of the factors that influence the climate.

### 3 Sun Angles Influence Sensor Performance

The angle of the sun has a big influence on the amount of sunlight that enters the cabin. In order for the solar sensor to be used in a system preventing an increase of temperature it must be placed in a way allowing it to measure the intensity, the elevation and the azimuth, which is the horizontal angle, of the incoming sunlight. This chapter aims at highlighting the importance of measuring elevation, azimuth and intensity with the solar sensor, all solar sensors on the market cannot do this today.

The solar sensor in other vehicles, is usually positioned near the windshield in the middle of the dashboard, which implies that for most sun angles the sensor will be sunlit. (Mårdberg, 2012) In some cases when the sun is highly elevated the sensor will measure a higher sun load entering the cabin than what actually enters the cabin, this due to shielding effects by the roof and other components of the vehicle. Hence, there can be a large difference between the measured sun load and the actual load that enters the cabin.

In order to calculate the sun load that enters the cabin, the total window area through which the sunlight enters the cabin must be calculated. This area is the window area projected on a perpendicular plane of the sun beams. The projected area is used due to that the sun load intensity is often given in the unit  $\text{W/m}^2$ .

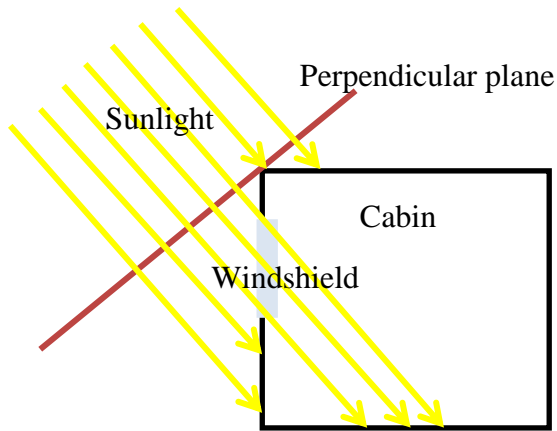


**Figure 4.** Sunlight entering the cabin.

The relative position of the sun with respect to the windshield is determined by a horizontal and a vertical angle, called azimuth and elevation respectively. Since it is complicated to take both into account simultaneously their impact has been evaluated separately. However, for this case it is considered valid since the aim is to obtain the largest possible projected area and to evaluate the importance of measuring the position of the sun. The largest projected area was used in the simulations of the heat balance of the cabin, in order to get the worst case scenario.

To calculate the largest projected area the first step was to keep the elevation angle at zero degrees and to vary the azimuth angle. In the next step the azimuth was kept constant at zero degrees and the elevation angle was varied.

### *Projected window area depending on azimuth*

To simplify the calculation of the projected areas depending on azimuth a simple sketch was made in the CAD software Inventor. A sketch of a cabin made in CAD is shown in figure 5.

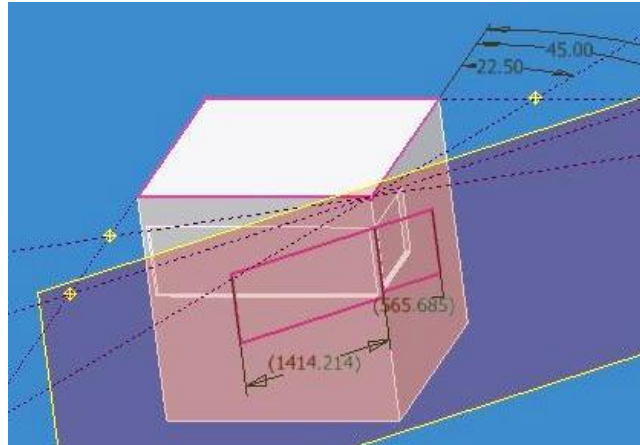


**Figure 5.** The windows projected area on a plane perpendicular to the sun beams.

The area depending on the azimuth of the sun when it is positioned close to the horizon can be calculated according to equation four.

$$A = H * W * \cos(90 - \alpha) + h * w * \cos(\alpha) \quad (4)$$

Where  $A$  is the projected area,  $H$  is the height of the windshield,  $W$  is the width of the windshield  $\alpha$  is the azimuth in this equation defined as zero when perpendicular to the side of the truck,  $h$  is the height of the side window and  $w$  is the width of the side window. The function was plotted in Matlab to obtain the largest total projected window area.

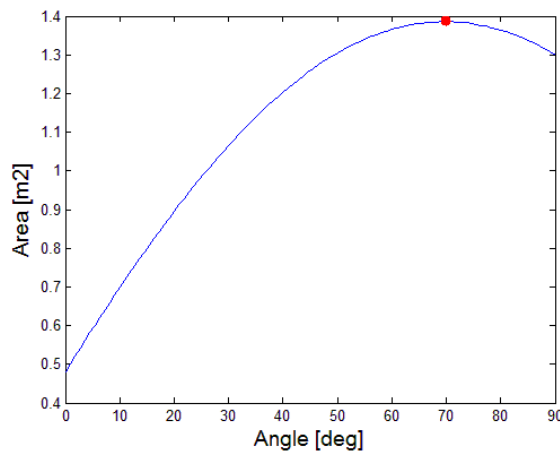


**Figure 6.** The projected area of the windows depending on azimuth angle.

The largest projected area depending on the azimuth angle was calculated to be  $1.39 \text{ m}^2$  as seen in the graph above, which occurs when the azimuth angle of the sun is  $70^\circ$  and when the

elevation angle is close to zero. This maximum area of 1.39 m<sup>2</sup> was later on used in the simulations.

*Projected window area depending on elevation*

The sun load entering the cabin is calculated according to equation five.

$$\begin{aligned} & \text{Entering Sun Load [W]} = \\ & = \text{Outside Sun Load [W/m}^2\text{]} * \text{Projected Window Area [m}^2\text{]} * \\ & * \text{Transmission Factor of the Windows [%]} \end{aligned} \quad (5)$$

Transmission is given in percentage and represents the amount of sunlight transmitted through the material. However, the sensor measures the sun load or the sun load intensity on the sensor and not the actual sun load entering the cabin. The sun load measured by the sensor is given by equation 6.

$$\begin{aligned} & \text{Measured Solar heat Load [W]} = \\ & = \text{OutsideSunLoad[W/m}^2\text{]} * \text{Transmissionfactorofthewindow[%]} * 1[m}^2\text{]} \end{aligned} \quad (6)$$

The transmission factor was 89 % for the windshield and 76 % for the side windows. (Volvo GTT, 4) The total transmission factor was a weighted factor of the transmissivities of the two glass constants with regard to the areas of the windows. In equation 6 the outside sun load is multiplied with the unit meters, to make it possible to compare the results. However, in reality the output signal of the sensor is neither in watt nor watt per square meters, it is in voltage. With help from a transfer function, see appendix A, it is possible to calculate the corresponding amount of watt or watt per square meters for a given sensor signal.

In table 1 the actual sun load outside, the measured sun load and the entering sun load with regard to several cases of projected window areas are shown.

*Table 1. The sun loads depending on projected area of the window.*

Projected Area [m <sup>2</sup> ]	Outside Sun Load [W/m <sup>2</sup> ]	Entering Sun Load [W]	Measured Sun Load [W]
1.30	600	694.2	534
1.20	600	641.4	534
0.92	600	490.9	534
0.50	600	265.7	534

The case of a projected area of  $0.5 \text{ m}^2$  represents the sun with a high elevation angle and an azimuth angle close to zero. In this case the difference between the measured sun load and the actual load entering the cab is substantial. The sensor indicates in this case that there is a 534 W load that enters the cabin, however the actual load entering the cabin is 266 W. In figure 7 a schematic sketch of this case is shown.

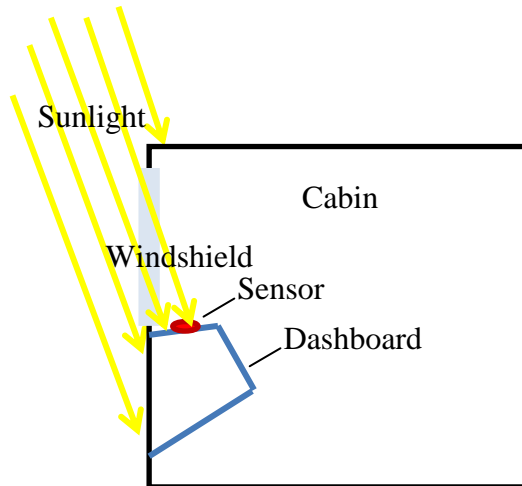


**Figure 7.** Only a small sun load enters the cabin, but the sensor is hit by the sun and senses a high sun load.

However, the difference between the measured and the entering sun load may not be this large if the control system is designed to consider the impact of the elevation angle of the sun and the cabin geometry is taken into account.

Another possible solution is to design the casing of the sensor so that the casing has a shadowing function of the sensing element when the sun is highly elevated. This additional casing can be constructed to represent the cabin geometry in order to shadow the sensing element in the same way as the roof shadows the interior of the cabin. (Mårdberg, 2012) However, the negative aspect of a casing with shadowing effect is that it is inflexible for changes regarding the position of the sensor and the geometry of the cabin.

The recommendation is to use a sensor that can measure elevation, azimuth and intensity of the sunlight. In addition design a control system which can calculate the sun load entering the cabin. It is considered that the design of shielding hardware aggravates the possibility of small changes of the position of the sensor which might be needed for different truck models

## 4 Simulation of the Heat Balance

In order to find the required accuracy and time constant of the solar sensor a simulation of the heat balance of the cabin was performed. In the simulations it was assumed that the required accuracy of the temperature control system is  $\pm 1$  °C. The model used for the simulation is originally used to simulate the heat balance of buildings, but with some modifications the model was used to simulate the heat balance of the cabin of a truck. Calculations were done by hand to confirm the results from the simulations, see appendix D. The equations used in the model are presented in appendix I.

### 4.1 Assumptions

It was decided that the simulation of the heat balance should be executed for the worst case scenario in order to find the design parameters of the sensor. The worst case scenario was defined according to the following assumptions:

- There are no winds affecting the convection on the outer surface of the truck, free convection is assumed. This assumption lowers the total heat transfer coefficient of the walls of the cabin, due to smaller heat transfer by convection.
- The required accuracy of the temperature control is  $\pm 1$  °C, as it was assumed that the human body does not feel smaller temperature changes.
- The heat transfer properties of the walls were taken from various tables, see appendix E, the tables represents the heat conductive parameters of materials similar to those used in the walls of the truck.
- It is assumed that no light entering the cabin is going out through other windows.
- It is assumed that the sun load entering the cabin directly heats the air in the cabin, not via heated surfaces in the cabin which slowly emit heat to the air. This makes the air temperature increase faster, to get a worst case scenario while simulating.

Other assumptions made were:

#### *Equivalent outside temperature*

When the cabin of the truck is sunlit there is a maximum of three sides of the cabin that are sunlit simultaneously. The equivalent outside air temperature was used to compensate for the increased temperature on the sides that were sunlit. The equivalent temperature was calculated according to equation seven.

$$T_{eq}^{eq,sun} = T_o + \frac{\alpha_{sun}}{\alpha_E} * I_{sun} \quad (7)$$

Where  $T_o$  is the outside temperature in °C,  $\alpha_{sun}$  is the color dependent absorptivity factor,  $\alpha_E$  is the convection coefficient in W/(m<sup>2</sup>K) and  $I_{sun}$  is the sun load in W/m<sup>2</sup>. (Petersson, 2009) In equation seven the sides that are sunlit are represented by the lower case index *eq*. For the sides of the cabin that are not sunlit the real Outside Air Temperature (OAT) is used.

#### *Heat from the engine*

It is complicated to approximate the amount of heat from the engine entering the cabin trough the floor of the cabin. A qualified assumption is that there is an increase of the cabin floor

temperature by 15 °C during normal driving due to the heat contribution from the engine. (Fellbom, 2012) In this assumption a heated cabin floor area of 0.75 m<sup>2</sup> and an outside temperature of about 20 °C were used. It is also assumed that the temperature in the cabin is 21 °C and the convection coefficient of the cabin floor was chosen to be 25 W/m<sup>2</sup>K to represent a value between natural convection and forced convection. (Fellbom, 2012) The heat contribution from the engine can be calculated according to equation8.

$$Q_{engine} = A * h_{convection} * \Delta T = \\ = 0.75 \text{ m}^2 * 25 \frac{\text{W}}{\text{m}^2\text{K}} * 15 \text{ K} = 281.3 \text{ W} \quad (8)$$

Where Q<sub>engine</sub> is the heat contribution in [W], A is the floor area in [m<sup>2</sup>], h<sub>convection</sub> is the convection coefficient in [W/m<sup>2</sup>K] and ΔT is the increase of the floor temperature due to the heating.

## 4.2 Accuracy

Since it was assumed that a person can feel a temperature change of one degree celsius or more, it was decided that the sun load giving rise to an increase of one degree celsius of the compartment air would provide the accuracy required for the feedforward system including the sensor.

### 4.2.1 Procedure

When simulations were done to determinate the desired accuracy of the solar sensor, the temperature of the air leaving the CCS, here called the *supply air temperature*, was kept constant and the supply air flow rate was changed. For the first simulations a supply air flow rate of 0.06 m<sup>3</sup>/s was chosen, which can be considered as reasonable. (Fellbom, 2012) Once the supply air flow rate was chosen the supply air temperature was tuned in to reach a steady state temperature of 21 °C in the compartment air. After steady state was reached the sun load was added in a step function and thereafter the load was tuned iteratively in order to find for which sun load the temperature of the compartment air would rise to a steady state of 22 °C.

The criterion was that the solar sensor and the feedforward control system should manage to detect and prevent an increase of one degree celsius or more, therefore the simulation was performed without the feedback control system otherwise present in the air control system. In normal driving both the feedforward and feedback systems are active.

In order to find the required accuracy of a solar sensor different sun loads were applied to the cabin for different flow rates of the supply air. The step of entering solar radiation and the response in temperature are shown in figure 8 below.

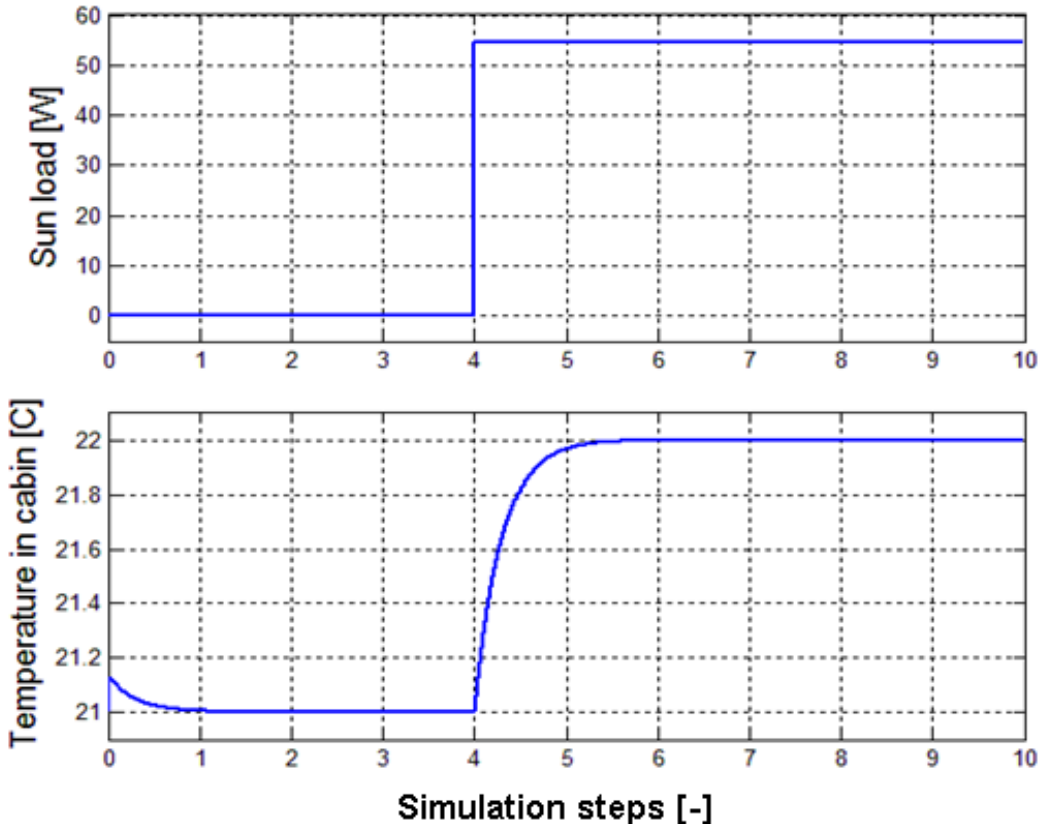


**Figure 8.** Upper figure: A sun load is added in a step function. Lower figure: The air in the cabin is heated due to the sun load applied. In this case a supply air flow rate of  $0.07\text{m}^3/\text{s}$  is used.

At the start of the respond signal in figure 8 there is a small slope of the curve which is due to some initial boundary values and has no impact on the results of the simulations.

The sun load into the cabin, which results in the temperature rise from  $21\text{ }^\circ\text{C}$  steady state to  $22\text{ }^\circ\text{C}$  steady state, depends on the supply air flow rate. In the table 2 the step of entering sun load resulting in an increase of one degree celsius in the simulations are presented. The step in entering sun load is the amount of heat transmitted to the cabin air. The inputs that were kept constant during the simulations were:

- The initial temperature of the air in the cabin of  $21\text{ }^\circ\text{C}$ .
- The outside air temperature of  $15\text{ }^\circ\text{C}$ .
- The cabin color was white.
- One person was assumed to be inside the cabin.

As mentioned above the equivalent outside temperature varies with the sun load. The step of sun load entering the cabin resulting in an increase from  $21\text{ }^\circ\text{C}$  to  $22\text{ }^\circ\text{C}$  in the cabin varies linearly with the flow rate of the supply air. More information about this cooling potential behavior can be found in appendix F.

**Table 2.** The steps of sun load entering the cabin for different supply air flow rates.

Supply Air Flow Rate [m <sup>3</sup> /s]	0.04	0.05	0.06	0.07
Equivalent OAT [°C]	15.78	15.89	15.99	16.09
Step of Sun Load Entering the Cabin [W]	39.2	44.3	49.5	54.65

## 4.2.2 Results

The results show that if the temperature in the cabin is at steady state 21 °C with a steady supply air flow rate of 0.04 m<sup>3</sup>/s, a sudden energy inflow from the sun of 39.2 W will result in a new steady state temperature inside the cabin of 22 °C, when the volume airflow is kept at 0.04 m<sup>3</sup>/s. If the rate of the supply air is 0.05 m<sup>3</sup>/s then the step of solar heat gain resulting in an increase of one degree celsius of the air in the cabin is 44.3 W. For each supply air flow rate case the supply air temperature was kept constant during the simulations.

### Cabin color and outside temperature

It was tested if the color of the cabin would impact the result. The color of the cabin is considered in the equivalent outside temperature. It was seen that the cabin color does not impact the result. For the same supply air flow rate the results for a white and black cabin gained from the simulation were equal. This is due to that for a given rate of the supply air, the supply air temperature is tuned in so that the temperature inside the cabin is 21 °C steady state. When the temperature is constant over time it is an equal amount of energy that enters the cabin that is cooled off. In the case of a black vehicle a greater cooling load is needed to keep the temperature at 21 °C. However, the influx energy from the sun resulting in a temperature increase of the compartment air of one degree celsius is equal for the white vehicle. To reach energy balance the same amount of heat must be cooled off to compensate for the sudden sun load, as in the white cabin case. But in total the cooling load in a black cabin is larger.

It was also tested whether different outside temperatures would affect the results and it did not, which is due to the same reasons as with the preceding case.

**Table 3.** The values for the solar radiation and the measured sun load for different supply air flow rates.

Supply Air Flow Rates [m <sup>3</sup> /s]	Step of Entering Solar Radiation [W]	Weighted Transmission Factor [%]	Measured Sun Load [W/m <sup>2</sup> ]	Solar Radiation (Outside) [W/m <sup>2</sup> ]
0.04	39.2	87.5	28.29	32.34
0.05	44.3	87.5	31.97	36.55
0.06	49.5	87.5	35.72	40.84
0.07	54.7	87.5	39.44	45.09

The results in table 3 were calculated using equations presented in appendix G. In table 3 the largest projected area of  $1.39 \text{ m}^2$  were used to transform the step of solar radiation from W to  $\text{W/m}^2$ .

The area of approximately  $1.39 \text{ m}^2$  is the largest possible projected area and is therefore used for dimensioning. The supply air flow  $0.05 \text{ m}^3/\text{s}$  was chosen, since an air flow of  $0.05\text{-}0.06 \text{ m}^3/\text{s}$  is usual while driving. (Fellbom, 2012) With these assumptions the accuracy is required to be  $\pm 44.3 \text{ W}$  or  $\pm 32 \text{ W/m}^2$ , this is the accuracy for the entire feed-forward system. A part of the accuracy required for the feedforward system will have to be allocated to the solar sensor to get its accuracy.

### 4.2.3 Required Solar Sensor Accuracy

To be able to allocate a part of the required accuracy of the feedforward system to the solar sensor, other accuracies in the feedforward system must be considered. Other than the solar sensor also the temperature sensor that measures the supply air temperature and the supply air flow rate are sources of inaccuracy. The supply air temperature sensor has an accuracy of about  $\pm 1 \text{ }^\circ\text{C}$ . (Mårdberg, 2012) The supply air flow rate can differ  $\pm 20 \%$  due to different pressure losses depending on through which ducts the air is distributed and due to inaccuracy of the flaps distributing the air. (Mårdberg, 2012)

In order to allocate the accuracy of the solar sensor from the  $44.3 \text{ W}$  of acceptable error of the feedforward system, the error of the volume flow control and the temperature measurement must be recalculated to energy. The recalculation is performed according to equation nine.

$$Q_{\text{case}} = x * V * \rho * c_p * (T_{\text{cab}} - (T_{\text{in}} + y)) \quad (9)$$

$Q_{\text{case}}$  is the cooling load [W],  $V$  is the supply air flow rate [ $\text{m}^3/\text{s}$ ],  $c_p$  is the specific heat capacity of air [ $\text{J/kg K}$ ] and  $\rho$  is the density of air [ $\text{kg/m}^3$ ].  $T_{\text{cab}}$  is the required temperature in the cabin, in this case  $T_{\text{cab}}$  is  $21 \text{ }^\circ\text{C}$ , and  $T_{\text{in}}$  is the supply air temperature [ $^\circ\text{C}$ ]. The parameters  $x$  and  $y$  represent the inaccuracy of the supply air flow rate and the inlet temperature respectively.

The cooling load needed for the energy flows to be balanced, in the dimensioning case with a volume flow of  $0.5 \text{ m}^3/\text{s}$ , is  $x = 1$  and  $y = 0$ , resulting in a needed cooling load of  $170.1 \text{ W}$  called  $Q_{\text{needed}}$ .

Since the measured air flow can deviate from the actual air flow with up to  $20 \%$  the value of factor  $x$  from equation nine can vary from 0.8 to 1.2. The factor  $y$  from the same equation can vary between -1 to +1 due to that the supply air temperature sensor can have an inaccuracy of one degree Celsius. These parameters provide four extreme cases presented in the table 4.

**Table 4.** The cooling load in for extreme cases.

Case	$Q_{\text{case}} [\text{W}]$	$Q_{\text{needed}} - Q_{\text{case}} = \text{Error} [\text{W}]$
x=1.2, y=+1	132.8	38.17
x=1.2, y=-1	277.5	-106.55
x=0.8, y=+1	88.5	82.43
x=0.8, y=-1	185.0	-14.05

In the first case where  $x = 1.2$  and  $y = +1$ , the accuracy of the sensor is required to be:

$$44.30 \text{ W} - 38.17 \text{ W} = 6.13 \text{ W}$$

Where 44.3 W is the accuracy needed for the entire feedforward system and 38.17 W is the difference between the required cooling load and  $Q_{\text{case}}$  shown in the third column in the table above.

This accuracy of  $\pm 6.13 \text{ W}$  is smaller than needed in the last case where  $x = 0.8$  and  $y = -1$ . In the case where  $x = 1.2$  and  $y = -1$ , the cooling load is larger than required. However the simulations showed that if the cooling load is 106,55 W more than needed and the sensor measures 6.13 W wrong, which gives the total error of 112.55 W extra cooling. Then the temperature without any sun load applied is 19.99 °C and when the sun load is applied 20,98 °C. This is approximately within the range  $\pm 1$  °C from 21 °C. So an accuracy of 6.13 W for the solar sensor will also handle this case. In the case when  $x = 0.8$  and  $y = -1$ , the cooling load is too small and the temperature after the sun load is applied is 23.16 °C. This case is out of reach for the feed forward system, since the total allowed error is 44.3 W which is much smaller than 82,43 W. In this case it is needed to rely on the feedback system.

Hence the required accuracy of the solar sensor is  $\pm 6.13 \text{ W}$ . The same accuracy expressed in  $\text{W/m}^2$  will then be  $\pm 6.13 \text{ W}$  divided by the window area of  $1.39 \text{ m}^2$  which is  $\pm 4.42 \text{ W/m}^2$ .

### 4.3 Time Constant

The following simulations were performed to find the time constraint, which is the time it takes for the feedforward system to react to the incoming load and to prevent a temperature increase bigger than one degree celsius. This time constraint is needed to calculate the time constant of the solar sensor. The sensor measuring the cabin temperature is slow compared to a solar sensor, therefore the sun load giving rise to 1 °C has to be handled by the feedforward control system. This is why no feedback system is used in the simulation. The system, including the supply air flow etc., is tuned in to be stable at 21 °C. After that an assumed sun load is applied and the time when the temperature has increased to a steady state of 22 °C is measured.

The time constraint in this case will be for the entire feedforward system. This includes the time delay for the fan to change its speed, the time it takes for the supply air temperature sensor to measure and the solar sensors time constant. A part of the time constraint for the feedforward system will have to be allocated to the solar sensor in order to get the time constraint, time constant and rise time of the solar sensor.

### 4.3.1 Procedure

Solar radiation cases were chosen and recalculated to see how much energy comes in to the cabin for each sun load case. This was done using the formula below:

$$\begin{aligned}
 \text{Entering Sun Load} = \\
 = \text{Solar Radiation} * \text{Maximum window area hit by the sun} * \\
 * \text{transmission factor of the windows}
 \end{aligned} \tag{10}$$

The largest projected window area of  $1.39 \text{ m}^2$  was used to simulate the worst case scenario.

**Table 5.** Solar radiation outside the vehicle and the sun load entering the vehicle.

Solar Radiation (Outside) [W/m <sup>2</sup> ]	Entering Sun Load [W]
700	848
800	970
900	1091
1000	1212
1100	1333

The sun load was added in a step function and the time it took for the air temperature to increase one degree Celsius in the cabin was measured. The case with a sun load of  $800 \text{ W/m}^2$  outside is shown in figure 9.

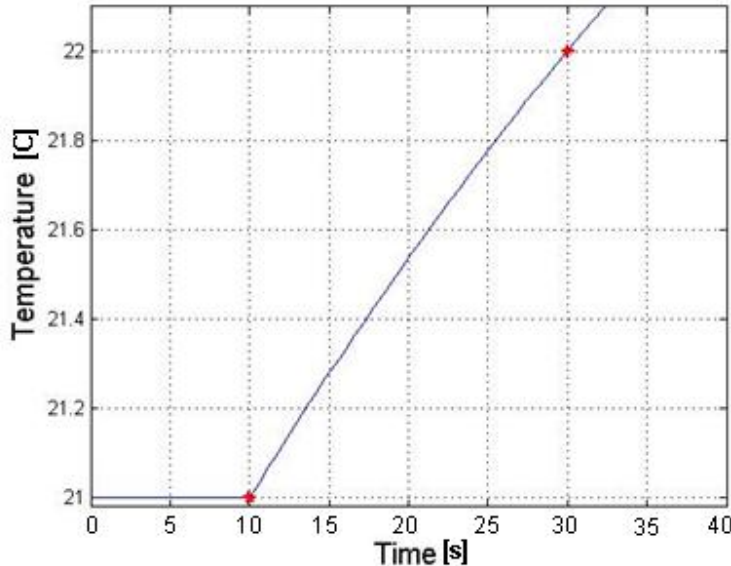


**Figure 9.** The temperature increases in the cabin over time. The time between the two red dots in the figure represent the time in which the feed forward system must react.

### 4.3.2 Results

In table 6 below, the time it takes for the temperature to increase from 21 °C to 22 °C for different sun loads is shown.

**Table 6.** Solar radiation outside the vehicle, the sun load entering the vehicle and the time it takes for the cabin temperature to increase one degree.

Solar Radiation [W/m <sup>2</sup> ]	Entering Sun Load [W]	Time [s]
700	848	23
800	970	20
900	1091	17
1000	1212	15
1100	1333	14

As seen in the table several cases were simulated, the cases with a solar radiation of 1000 W/m<sup>2</sup> or higher may however be seen as rather unlikely. (SMHI, 2007) The largest projected area of the windows were used in the simulation which implies that the elevation of the sun is rather low which in turn implies a lower sun intensity compared to when the sun has a high elevation angle. Hence, the dimensioning case chosen was the case with solar radiation intensity of 900 W/m<sup>2</sup>. The chosen case provided a time constraint for the whole feed forward system of 17 seconds.

#### *Allocation of time constraint to the solar sensor*

In order to allocate the time constraint to the solar sensor the time constraints of the other parts of the feedforward system was evaluated. The slowest component of the feedforward system is the air temperature handling, it can take up to approximately 15 seconds for the AC-system to change the temperature of the air coming into the cabin. It also takes a few seconds for the control unit to calculate the required temperature and a few seconds for the air distribution flaps to adjust to the correct position, however it is assumed that this would happen simultaneously so it is fair to state that it takes 15 seconds for the entire feedforward system, except for the solar sensor, to reach the required state. (Mårdberg, 2012) The time constraint for the solar sensor was calculated according to equation 11.

$$\begin{aligned} \text{Sensor time constraint} = \\ = \text{time constraint whole feed forward system} - \text{time it takes for air handing} \quad (11) \end{aligned}$$

This resulted in a time constraint for the sensor of two seconds.

### 4.3.3 Required Solar Sensor Time Constraint

To be able to use this time constraint when comparing sensors either a time constant or a rise time parameter is needed. The time constant is defined as the time when 63 % of the final value is reached while the rise time parameter is defined as the time when 90 % of the final value is reached. (Lennartson, 2002) The response signal of the sensor is approximated to be linear and hence the time constant and rise time is approximated to be 63 % and 90 % of the two seconds

allocated to the solar sensor. Hence, the time constant is calculated to be 1.26 seconds and the rise time is 1.8 seconds.

## **4.4 Summary, Simulation**

The required accuracy of the solar sensor was calculated to be 6.13 W or  $4.42 \text{ W/m}^2$ , and is recommended to be approximately  $\pm 6 \text{ W}$  or  $\pm 4.5 \text{ W/m}^2$  respectively. The dimensioning case chosen was with a window area of  $1.39 \text{ m}^2$  and airflow of  $0.5 \text{ m}^3/\text{s}$ .

The time constant is recommended to be between one and two seconds, calculated to be 1.26 seconds. The corresponding rise time is about two seconds, calculated to be 1.8 seconds. The dimensioning case chosen was with a solar radiation intensity of  $900 \text{ W/m}^2$ .



## **5      Benchmark**

A benchmark was performed in order to map the available sensors on the market. There are several ways of describing what a benchmark is, central is that it involves comparing a company, product or service with its competitors. A benchmark can be done to see how competitive the company or product is or to localize where the company should focus their improvements. (Stapenhurst, 2009) In the thesis a benchmark was performed to map the sensors and manufacturers on the market.

### **5.1    Method**

The American Productivity & Quality Center (APQC) has created a methodology for benchmarking, where four phases are identified. (Coers, 2001) In the first phase the area or product in need of improvement is localized. The first step also includes the definition of a clear scope of the study, the selection of the team that will perform the benchmark and to find measuring parameters for the existing process or product. (Coers, 2001)

When the first step is performed the partners of the benchmark should be selected. In the second phase of a benchmark the chosen participants should be contacted and a list in which the responses of the manufacturers can be stored and structured should be developed. This contact with the manufacturers can be performed by written interviews, by telephone interviews or by visits. (Coers, 2001)

The third phase of the benchmark is to analyze and report the results. In this step performance, best practices and gaps in performance are analyzed. In the fourth step it is important to focus on what leads to the best performance and to present this result. In the last phase improvements should be established, implemented and followed up (Coers, 2001).

#### **5.1.1   Procedure**

Volvo Group stated that it was of interest to find sensor parameters defining the performance of a sensor, in order for the sensor to fulfill the requirements set, which means that it would not be desirable to have a higher or lower quality of the sensor than would have to be needed.

The first step was to create a list of manufacturers for each sensor, the manufacturers were found by using search engines on the internet and by identifying existing suppliers within Volvo Group. The parameters used for the comparison of the solar sensor were the accuracy and the time constant, given by the simulations in chapter six. The fog sensor and the AQS sensor were not compared in the benchmark due to lack of information regarding the requirements of these sensors. However, the data provided from manufacturers of these two sensors are presented in appendix H.

At first existing sensor suppliers of other sensors and other highly interesting manufacturers were contacted. The solar sensor manufacturers were contacted first and later on the manufacturers of fog sensors and AQS sensors were contacted. The manufacturers were contacted via telephone and by e-mail. The sensor data sheets that were acquired from the manufacturers were evaluated,

structured and the functional parameters described in the sensor data sheets from the manufacturers were compared.

However, the functional parameters of the sensors described in the thesis are not always mentioned in the product datasheets. This can be due to that sensor data sheets often are made for marketing and sometimes specified for a specific customer, therefore all the required parameters may not always be present. The positive attributes are often highlighted and sometimes none of the functional parameters mentioned in this report are included in the data sheets. (Wilson, 2005)

## 5.2 Benchmark of Solar Sensor

Several manufacturers of sensors were contacted in order to perform a benchmark of the solar sensor, the fog sensor and the AQS sensor. The benchmark of the solar sensor is presented in this chapter and the benchmark of the fog sensor and the AQS sensor are presented in appendix H. It was revealed to be problematic to obtain complete data sheets from the sensor manufacturers. The data sheets that were obtained often did not include the same parameters, which resulted in a table of parameters where some of the parameters are missing. The solar sensor manufacturers contacted in the benchmark are presented in table 7.

*Table 7. Solar sensor manufacturers contacted and their response.*

Manufacturer	Response
Accel	Provided Data Sheets and Physical Tests
Behr Hella	Did not Provide Data Sheets
Casco	Provided Data Sheets
GE Measurement & Control	Provided Data Sheets
Honeywell	Did not have Solar sensors
Measurement Specialties	Did not Provide Data Sheets
PerkinElmer	Did not have Solar sensors Suitable for Vehicles
Polytec	Did not have Solar sensors Suitable for Vehicles
Preh	Did not Want to Participate
Sensata Technologies	Provided Data Sheets
Visteon	Did not have Solar sensors

In table 8 the data acquired from the sensor manufacturers is shown. The required accuracy of the solar sensor provided in chapter 6 was at first thought to be the primary parameter used for comparing the solar sensors. However, due to difficulties in acquire data sheets from manufacturers containing information about the accuracy of the solar sensors this was not possible. The manufacturers claimed that the accuracy is not specified in the data sheets because it is one of the parameters of the solar sensor that is custom made for each buyer. The manufacturers could not provide the data sheets of the sensors bought by other vehicle manufacturers due to that the data sheets are property of the buyer.

**Table 8.** Solar sensors and their functional parameters. \*Saturated at 700 W/m<sup>2</sup>.

	Accel – Dual Zone Sensor 1	Accel – Dual Zone Sensor 2	GE – Sun Load Sensor	GE – Single Solar Sensor	GE – Dual Solar Sensor	Casco – 3D Integrated Light Sensor	Sensata – Solar Watch Sensor	Sensata – Solar Twiligt Sensor
Measurement Range [W/m <sup>2</sup> ]	0 – 10000	0 – 700*	---	---	---	0 - 1500	---	
Evaluated Radiation Spectrum [nm]	---	400 - 1050	---	---	---	---	---	
Response time [s]	< 0.6	< 10 <sup>-2</sup>	45 * 10 <sup>-9</sup>	---	---	< 200 * 10 <sup>-3</sup>	Approx 4 *10 <sup>-9</sup>	10 <sup>-2</sup>
Non-linearity [%]	---	---	---	---	---	---	< 0.5	< 0.5
Operating Temperature [°C]	---	-40 to +105	-30 to +100	-10 to +100	---	-40 to +105	-40 to +115	-40 to +115
Storage Temperature [°C]	---	-40 to +105	-40 to +100	-25 to +90	---	---	-40 to +125	-40 to +125
Elevation Range [°]	180	---	---	---	---	10 to 145 (for azimuth 0°) 25 to 155 (for azimuth ±90°)	---	---
Elevation Accuracy [°]	---	---	---	---	At 45 ± 10	+ 9 / - 7	---	---
Azimuth Range [°]	360	---	---	---	---	-180 to +180	---	---
Azimuth Accuracy [°]	Symmetrical Response ± 5	---	---	---	---	± 10	---	---
Output Signal [mV]	---	---	58.8 ± 15 % to 20 %	58.8 ± 15 % to 20 %	58.8 ± 15 % to 20 %	---	---	
Operating Voltage Range [V]	5 ± 0.1	5 ± 0.1	---	---	---	---	5 ± 0.5	5 ± 0.5
Weight [g]	---	< 4 g	---	---	---	---	< 6	< 6
Package material [-]	---	---	---	---	---	---	PBT or PC+ABS	PBT or PC+ABS
Additional function [-]	---	---	---	---	---	Twilight Sensor	---	---

It is shown that the recommended response time given to be between one and two seconds by the simulations in chapter 6 is several magnitudes higher than the response times provided in the data sheets for most of the sensors. Therefore, when deciding upon which sensor to choose the response time is of minor importance since it is from this study shown that the required response time is more than fulfilled by the sensors reviewed in this benchmark.

In the benchmark some solar sensors with a 3D effect were presented, the 3D effect provides a measurement of the sun intensity entering from the back of the vehicle. The 3D effect solar sensors are presented by the manufacturers as the high technology choice. However, due to the design of the truck cabin a 3D effect solar sensor is excessive because of the shielding effects from the cabin walls. Some sensors were also possible to combine with a twilight sensor, measuring when it gets dark outside, to be able to regulate the control panel lighting.

### **5.2.1 Sensor Casings**

While choosing the solar sensor it is important to evaluate which casing of the sensor that is needed for the purpose. As could be seen in chapter 8 the casing has a significant impact on the performance of the sensor. A recommendation is to investigate the possibilities given by the sensor manufacturer Accel as they provide two different casings for their sensors depending on the requirements of the sensors.

Accel provides an infrared casing and a dimmed casing. The infrared casing only transmits infrared radiation, the transparency is close to 100 % in the infrared spectrum. The photo diode used in the sensor has a peak of sensitivity in the infrared region, therefore there is no need for amplification of the signal while using the infrared casing. Another positive aspect of the infrared casing is that the color is pitch black and it is not possible to see the interior parts when looking at the sensor, which is considered too look good. However, a drawback of the infrared casing is if there is a need to change the type of windshield it is necessary to correct the sensitivity either in the sensor or in the software. The dimmed casing also transmits in addition to the infrared radiation visible light between the range of 400 to 500 nm. One of the positive features of the dimmed casing is that the sensor can be integrated with an ambient light sensor, which senses when it is getting dark and the lighting in the control panel should be lit. The negative aspects are that if it is unwanted that the interior parts of the sensor are visible then it is needed to trim down the visibility of the sensor. This trimming result in a lower signal from the photo diode, it is up to five to ten times lower than with the infrared casing, therefore an amplification of the signal is needed.

### **5.2.2 Summary, Benchmark**

Overall it was seen that it is difficult to compare sensors by gathering data sheets from manufacturers. Sensors can be constructed in several ways with sensing elements in different configurations and different casings influencing the performance. For truck applications there is no need to measure sun load coming from the rear of the vehicle. Other than that it is difficult to recommend specific sensors. The aim was also to get prices of the sensors but this parameter is difficult for the manufacturers to supply so no comparison where possible. However it was seen that all the sensors examined had shorter time constant than required.



## 6 Test of Solar Sensors Developed by Accel

Tests were performed to evaluate the impact of the casing of the sensors and of a windshield used for products within the Volvo Group on the performance of a solar sensor, and in extension if the sensor can be placed outside the cabin. The tests were performed in cooperation with the Swedish and Lithuanian sensor manufacturer Accel.

Under guidance by Senior Director Arvydas Maldžiūnas and his colleagues the following tests were performed:

1. Transmissivity of the windshield depending on the wavelength of the light.
2. Transmissivity of two different sensor casings.
3. Influence of a windshield on the sensor signal.
4. Influence of a tilted windshield on the sensor signal.
5. A uniformity test of two sensor models.
6. Evaluation of the angular response of the sensors.

### 6.1 Equipment

The equipment used during the tests is presented below.

#### *USB4000 spectrometer*

In tests one and two a USB spectrometer called USB4000 was used. The spectrometer is made by Ocean Optics and is connected to a computer via a USB port to a computer. The software program SpectraSuite was used to display and store data when measuring with the USB4000 spectrometer. The SpectraSuite displays the result of the measuring in real time and saves the data in a format easy to export to Excel or MATLAB.

A reference measurement without the artificial light source was stored in SpectraSuite and was used to compensate for the external light sources present during the tests. The USB spectrometer has to be calibrated from time to time to measure accurate, a calibration was performed by the Accel personnel prior to the tests. The USB4000 spectrometer measures light within the wavelength range of 200 to 1100 nm. (Ocean Optics, 2006) For connecting the spectrometer optical fiber wires produced by Ocean Optics were used.



**Figure 10.** The USB4000 spectrometer.

#### *LS-1 Tungsten Halogen Light Source*

In the first test a light source produced by Ocean Optics was used. The light source provides a white light with wavelengths from 360 to 2000 nm. (Ocean Optics)

#### *Newport's Oriel Xenon Solar Simulator*

Tests two, three, four and five were performed with a more powerful light source. This light source was made by Newport and the light intensity can be adjusted and measured by a pyrometer. The lamp in the simulator emits a 5800 K blackbody like spectrum, the light is then filtered and the result is a constant output of solar like light beam lightening up about five times five cm<sup>2</sup> on the working plane. (Newport) A sketch of the solar simulator is shown in figure 11.

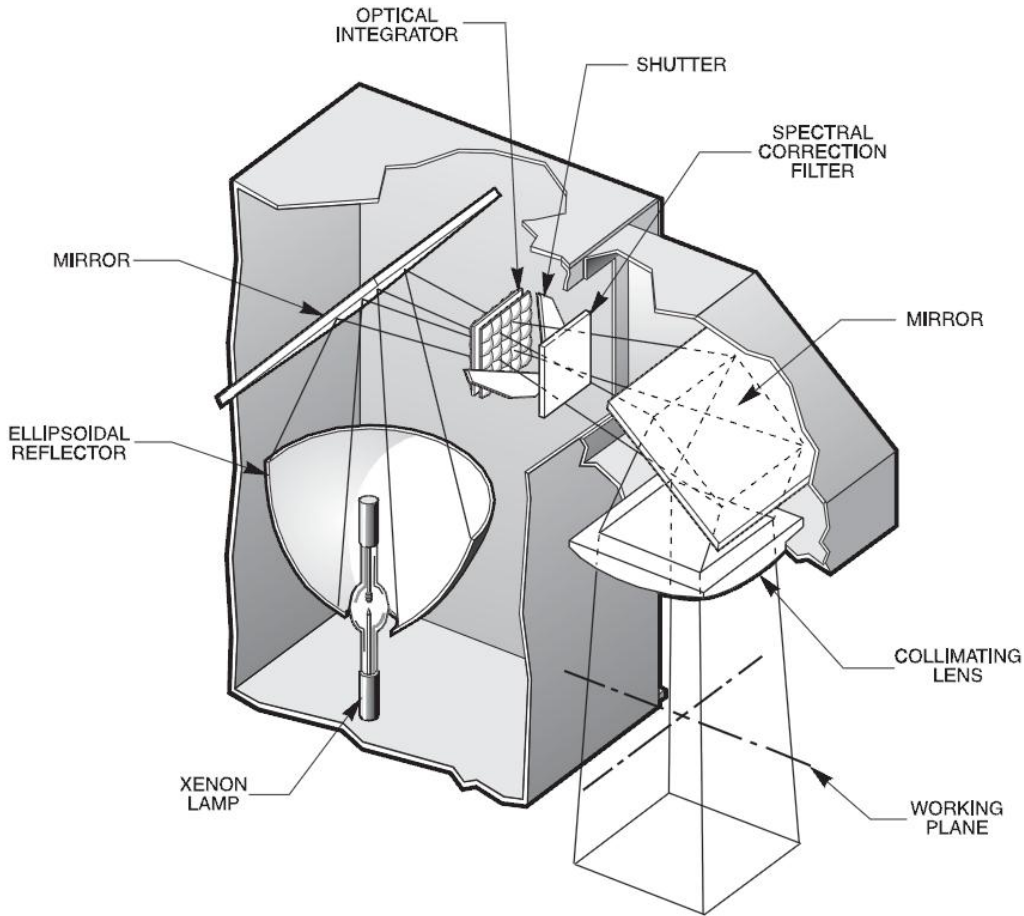


**Figure 11.** Source: (Newport). The solar simulator.

#### *IR sensor*

The so called IR sensor is one of the two sensors from Accel tested. This sensor is constructed by two sensing elements facing opposite directions. The IR sensor has a casing with high transmittance in the infra-red region of the spectra.

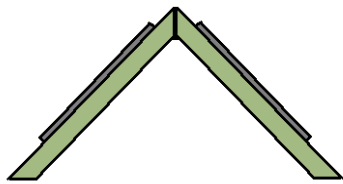


**Figure 12:** The picture shows a schematic sketch of the IR sensor from the side, where the grey parts are the sensing elements.

#### *Dim sensor*

The transmissivity of the Dim casing is approximately equal for all wavelengths. The Dim sensor consists of two sensor elements pointing in the same direction separated by a divider. The divider is simply a metal plate located in-between the sensing element. The divider shadows one of the sensing elements when the sunlight enters from the side. A schematic sketch is shown in figure 13, where the light gray part is the divider and the darker gray parts are the sensing elements.

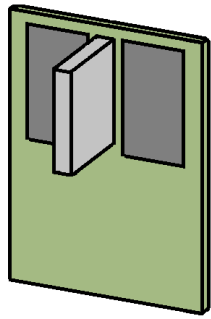


**Figure 13:** The picture shows a schematic sketch of the Dim sensor, where the darker grey parts are the sensing elements and the lighter gray part is the divider.

#### *Voltage Meter*

Two voltage meters were used to detect the signals from the two sensing elements in the sensors.

#### *Angular Response Apparatus*

An apparatus providing rotation and elevation of the sensor was used for the measurement of the angular responses of the sensors. The apparatus was developed and constructed by Accel.

In this thesis the sensors are named after their casings, the different techniques inside does not depend on the casing and both techniques could be used with both casings. Both sensors are produced by Accel and used by two different car manufacturers.

## 6.2 Source of Error

The tests were performed during a short amount of time, due to this there are some possible sources of error that might have occurred during the tests.

- During tests the optic fiber cables used might have been moved unnoticed and a movement of the cables would require a recalibration of the test.
- Background light might have changed during the tests due to external light sources may have been switched on or off.

- The sensors used for the tests might not always have been placed exactly in the center of the light beam of the light source.
- It was also difficult to ensure the mounting of the sensor to be completely horizontal.
- The sensor signals were measured with a volt meter and due to fluctuations of the signal it was difficult read the results with a high accuracy.

## 6.3 Tests Performed

The tests that were performed in cooperation with Accel are presented in this chapter.

### 6.3.1 Test 1 – Windshield Transmissivity

This test was performed to evaluate which wavelengths that are transmitted by the glass used in the windshields of the trucks.

In this test the USB4000 spectrometer and the LS-1 light source was used. An optical fiber cable was connected to the light source and the other end of the cable was mounted on a metal piece used to fixate the windshield glass. A similar metal piece was situated on the other side of the glass and another optical fiber cable was connected in that metal piece. The ends of the cables were facing each other with the windshield glass in between as can be seen in figure 14. The other end of the second cable was connected to the spectrometer. The LS-1 light source was activated and the test results were displayed and saved with the software SpectraSuite.

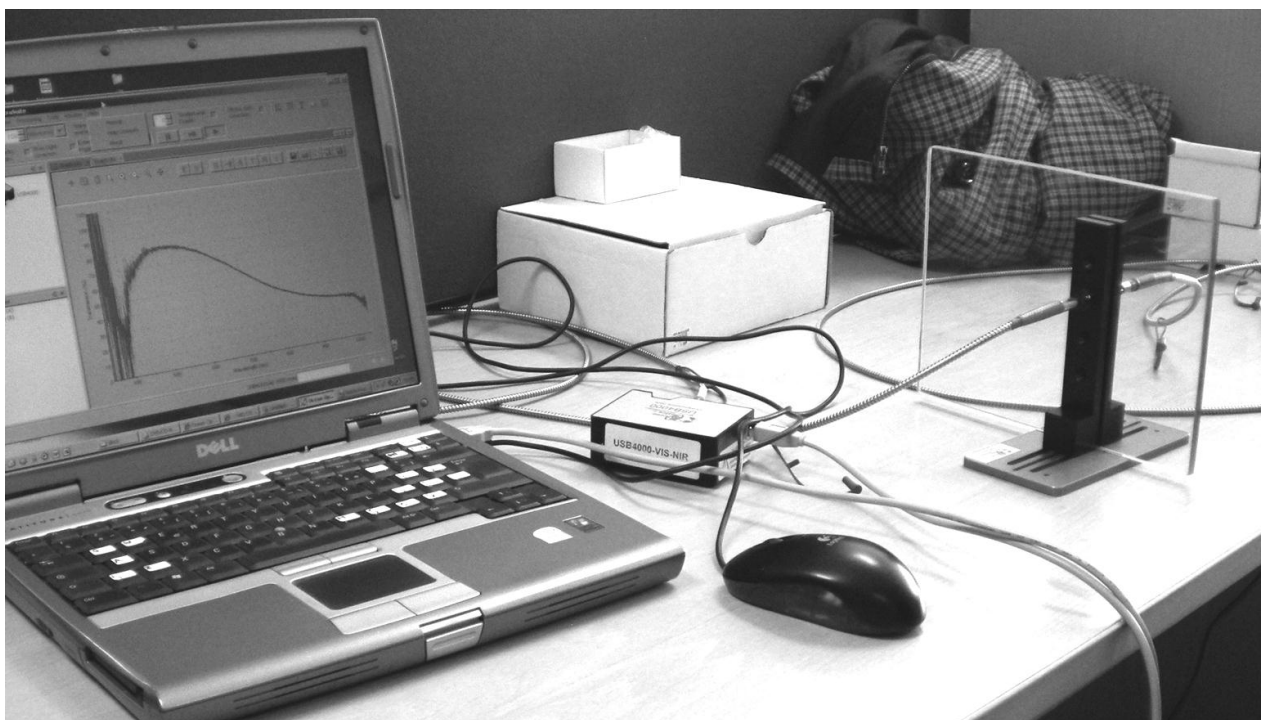


**Figure 14:** The picture shows the setup used in the first test.

In figure 15 below, the transmissivity of the glass is shown. The blue line represents the result from the test performed and the red line represents data provided by the supplier of the windshield glass. The light source in this case can only emit light in wavelengths from 360 nm and up, which explains the fluctuations of the blue line in the lower wavelength range.

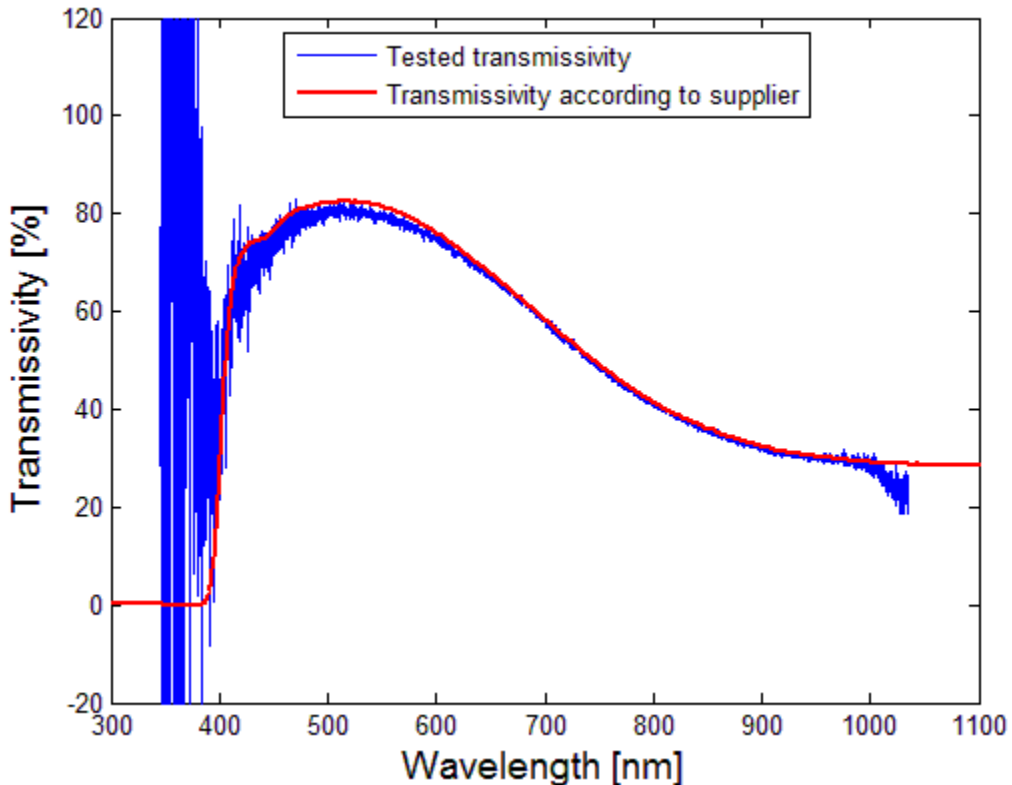


**Figure 15.** The figure shows the transmissivity of the windshield per wavelength.

The measured result of transmission confirms the data the supplier provided Volvo with. Small differences can however be seen in some wavelengths of the light, they may however originate from test equipment.

### 6.3.2 Test 2 – Transmissivity of Sensor Casing and Windshield

Test number 2 was performed to evaluate the influence of the spectral transmittance of the casing and the windshield. A question raised was whether it is possible to derive the same results from data given by the sensor casing supplier and the windshield supplier as from the physical tests.

To be able to measure transmittance through sensor casings a stronger lamp, Newport's Oriel Xenon Solar Simulator, was used. The optical fiber cable was connected to the USB4000 spectrometer and the end of the cable was placed under the Newport Oriel Xenon Solar Simulator. To evaluate the transmissivity of the casings they were placed on top of the optical fiber cable. The windshield was inserted between the light source and the sensor casing in order to evaluate its impact. The configuration of the test equipment can be seen in figure 16.

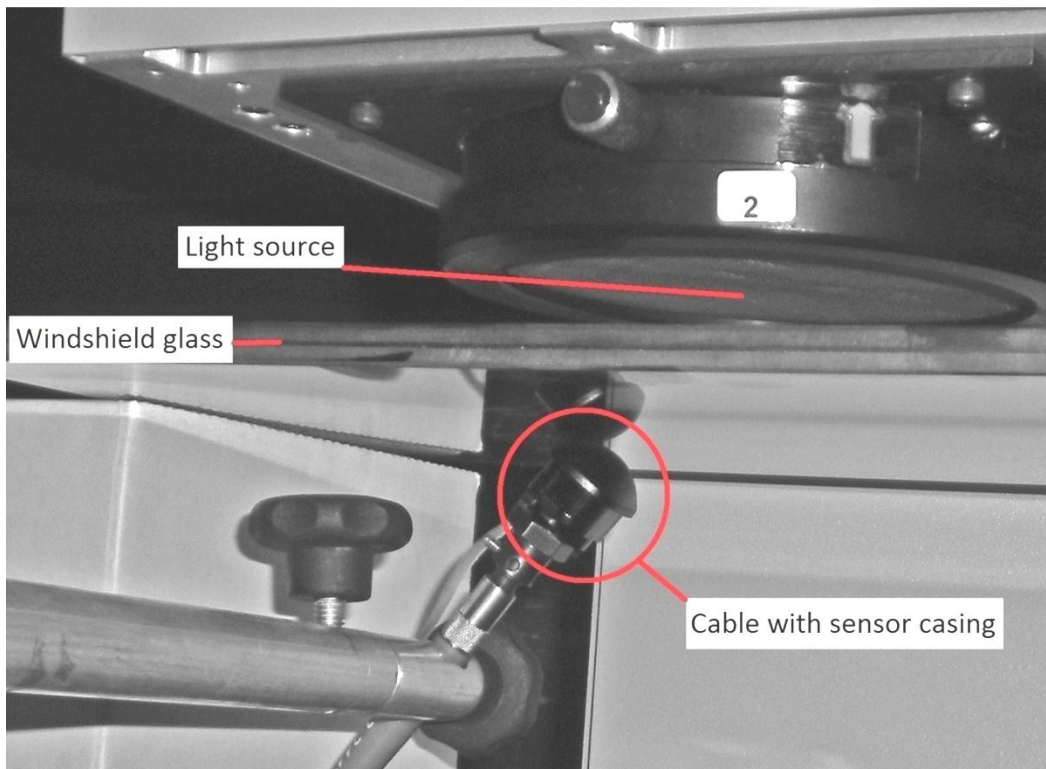


**Figure 16.** The setup used in test number two.

Figure 17 below shows the result of the tests. The red line represents the result from the tested transmissivity through the windshield and sensor casing. The blue line represents the calculated transmittance from the windshield supplier and with data for the sensor casings from Accel. The transmission was calculated according to equation 12:

$$\begin{aligned}
 & \text{Total transmission for a specific wavelength} = \\
 & = \text{transmission of the windshield for the wavelength} * \\
 & * \text{transmission of the casing for the wavelength}
 \end{aligned} \tag{12}$$

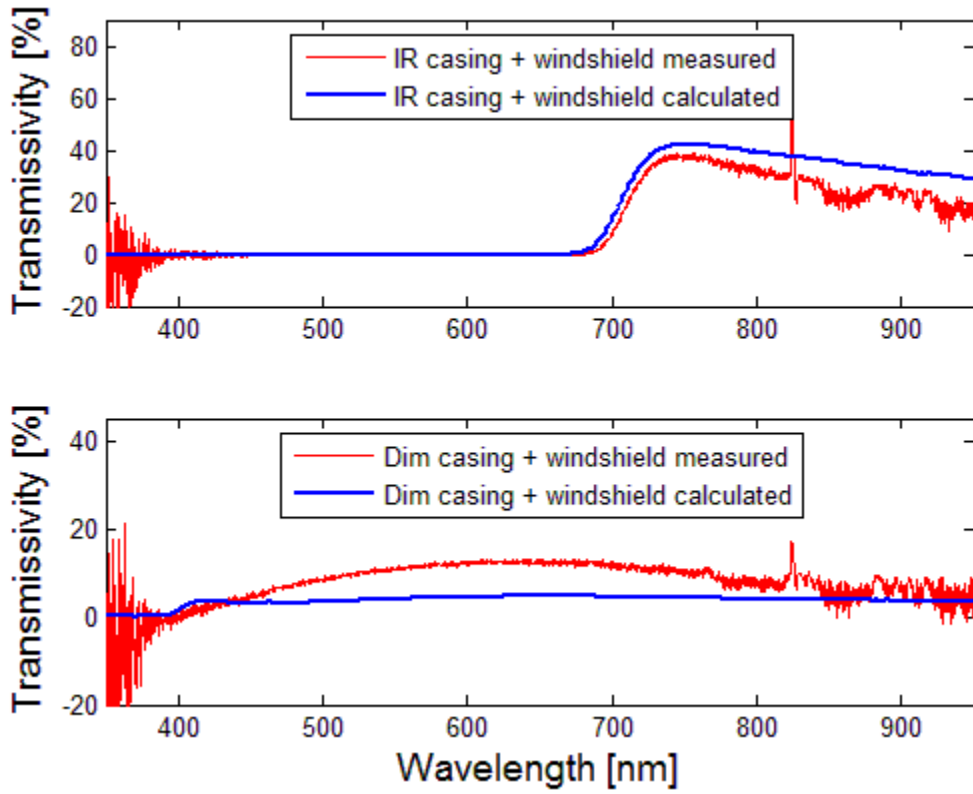


**Figure 17.** Tranmsissivity through the windshield and casing.

As seen in the picture the measured and calculated results differ. The calculated transmission with the Dim casing for example, is only just above 3.5 % in the wavelength of 500 nm, while the measured value is 8 %. These results show that it might be a good idea to test the combination of windshield glass and sensor casing in the truck before final tuning of the control system and not to rely on calculations.

### 6.3.3 Test 3 – Influence of a Windshield on the Sensor Signal

The signal from the sensors was measured with a voltage meter. The signals were measured for three cases with a light source, without a light source and with a light source plus the windshield glass. The three cases were examined for two different types of sensors. This test was performed in order to examine the influence of the windshield on the sensor output signal.

The tests were performed with the sun simulator used in test two. The light intensity was first set to be  $350 \text{ W/m}^2$  and then  $450 \text{ W/m}^2$ . The voltage from each sensor element was measured by two voltmeters, each displaying the signal from one of the sensing elements.

When the sun simulator was set to emit a light intensity of  $350 \text{ W/m}^2$  it was seen that the sensor signal voltage was about 37.8 % of the full signal for the Dim sensor. The IR sensor signal output with the windshield was about 34.5 % of the signal without the windshield. The signal from the

sensor when a windshield is used is compared with the full signal. The full signal is the difference between the measured voltage with and without a light source.

When the sun simulator was set to emit  $450 \text{ W/m}^2$  the Dim and IR sensor signal, while using the windshield, was 37.9 % and 34.8 % respectively, of the full signal. The test data are presented in table nine.

*Table 9. Sensor output signals.*

Cases		Light source: $350 \text{ W/m}^2$			Light source: $450 \text{ W/m}^2$		
		Voltage	Signal	percentage of full signal	Voltage	Signal	percentage of full signal
Dim sensor	No sun	4.67	0	-	4.67	0	-
		4.65	0	-	4.65	0	-
	Sun	3.57	1.10	100.0%	3.32	1.35	100.0%
		3.54	1.11	100.0%	3.30	1.35	100.0%
	Sun with glass	4.26	0.42	37.8%	4.16	0.51	37.9%
		4.23	0.42	37.8%	4.13	0.51	37.9%
IR sensor	No sun	4.51	0	-	4.51	0	-
		4.51	0	-	4.51	0	-
	Sun	3.31	1.20	100.0%	2.98	1.53	100.0%
		3.23	1.28	100.0%	3.07	1.44	100.0%
	Sun with glass	4.10	0.42	34.5%	3.98	0.53	34.7%
		4.07	0.44	34.5%	4.01	0.50	34.9%

There are two values for each case in the table, one value for each sensing element in the sensor.

According to the Volvo Group supplier of the windshield glass tested, the transmittance of the glass is said to be around 51 %, depending of which standard is used when calculating. (Volvo GTT, 2) As seen above this is not the difference in the signal from the sensor. This is due to that the sensors casing transmission is different for the different wavelengths, which is also true for the windshield as can be seen in figure 18. Most of the energy from the sun is within the wavelengths in the visual and IR region, which to a big extent is cut off while using the casings. The percentage 51 % represents the area under the blue line in the graph, while the combination of IR casing and glass represent the area under the red line.

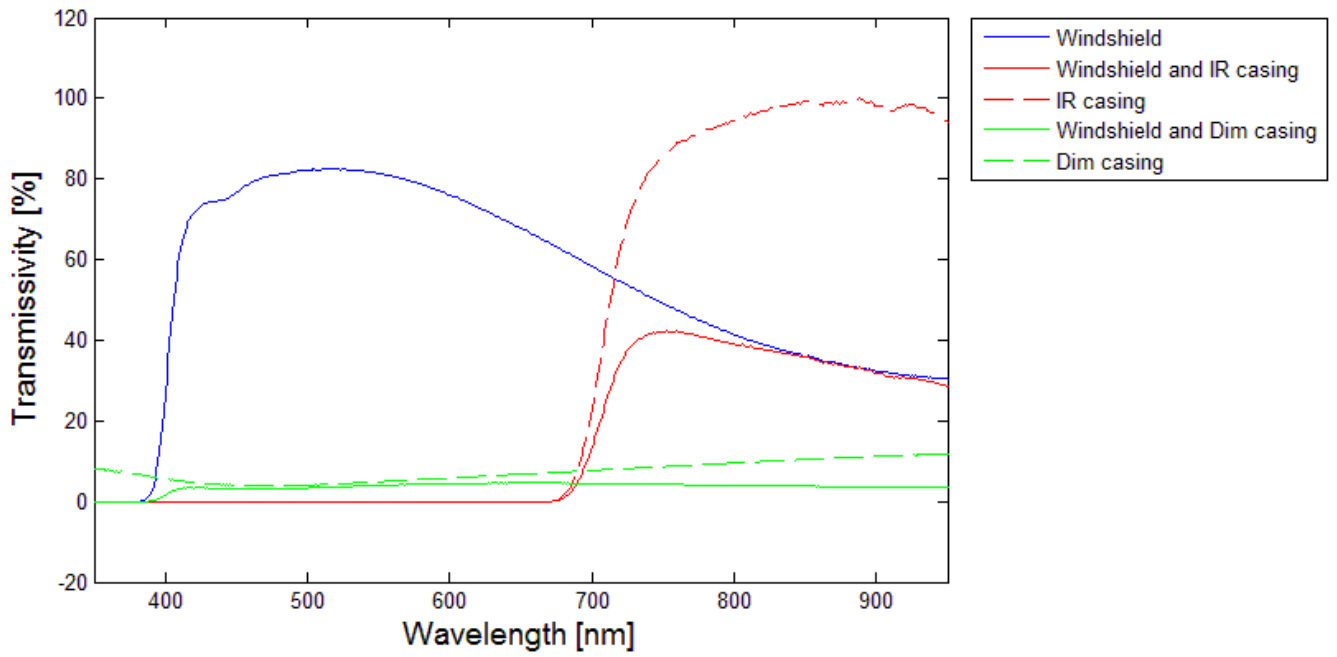


**Figure 18.** The calculated transmissivity of the windshield and casings.

The data in the graph is taken from the windshield supplier and Accel. The dotted lines represent the transmission of the casings without the sensors.

The sensor elements are probably also affecting the result, the sensor might measure with different accuracy for different wavelengths. So it is recommended that the sensor is tested with the glass it is supposed to be used with before tuning in the control system.

#### 6.3.4 Test 4 – Effect of a Tilted Windshield

Since the sun light in most cases is not perpendicular to the windshield the impact on the transmittance of a tilted glass was tested.

The tests were performed with the sun simulator used in test 2 and 3. The light intensity was set to be  $350 \text{ W/m}^2$ . The voltage from each sensor element was measured by two voltmeters. In the previous tests the windshield was placed horizontally above the sensing element, in this case one side of the glass was tilted upwards with angle of  $35^\circ$ . Due to equipment constraints this was the only angle tested.

It was seen that the sensor signal was a bit reduced when the glass was tilted. This is partly due to that more light is reflected by the windshield when it is tilted. However, the difference was quite small as can be seen in table 10.

Case		Signal	Percentage of full signal	Mean of the two elements	Difference	
Dim sensor	0°	0.438	40.04%	37.93%	3.19%	
		0.365	35.82%			
	35°	0.395	36.11%	34.74%		
		0.34	33.37%			
IR sensor	0°	0.389	34.58%	34.81%	3.51%	
		0.408	35.05%			
	35°	0.34	30.22%	31.31%		
		0.377	32.39%			

**Table 10.** Sensor output signals when the windshield glass is tilted

There are two values for each case in the table, one value for each sensing element in the sensor. When the glass is tilted the signal is 3.19 % and 3.51 % smaller for the Dim sensor and the IR sensor respectively.

The transmittance of the glass depends on the angle of the sun. The sensor placed inside the windshield measures what is coming into the cabin so it does not affect the performance of the sensor in a negative way. However, a sensor placed outside the cabin would not. Hence, it is recommended to place the sensor in the cabin.

### 6.3.5 Test 5 – Uniformity

A uniformity test was performed in order to evaluate the output range of six sensors of a batch. The test was performed in the same way as in test four. The sun simulator from Newport was used and two voltmeters.

The results are shown in figure 19, 20 and 21. The signal is shown on the y axis, observe that the y axis is cut off. The number of the sensor is shown on the x axis.

The IR sensor contained two sensing elements with an angle in between. Hence, when testing the IR sensor the sensor was first mounted with one sensing element facing towards the light source, then the sensor was turned and the other element was facing the light source. Figure 19 displays the signal when the elements were facing towards the light. In the next diagram the signal when the elements are pointing from the light source is displayed.

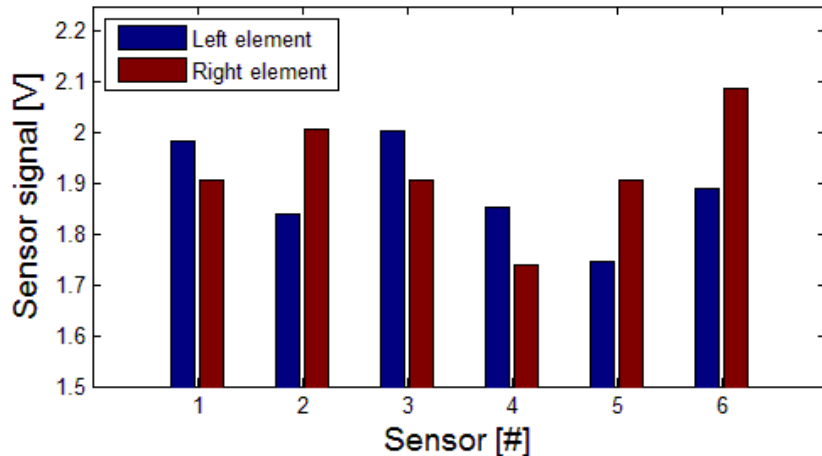


**Figure 19.** IR sensor, elements in light.

As seen in the diagram the signals from the sensor elements differ to some extent. The mean value of the signal when the elements are directly hit by the light is 1.9 V. The maximum signal is 109.4 % of the mean value signal and the minimum signal is 91.3 % of the mean value signal. The difference between the maximum and minimum signal is 16.6 % if defined according to equation 13.

$$\text{Difference [%]} = \frac{\text{maximum signal} - \text{minimum signal}}{\text{maximum signal}} \quad (13)$$

Below, the signal when the elements of the IR sensor are pointing from the light source is displayed.

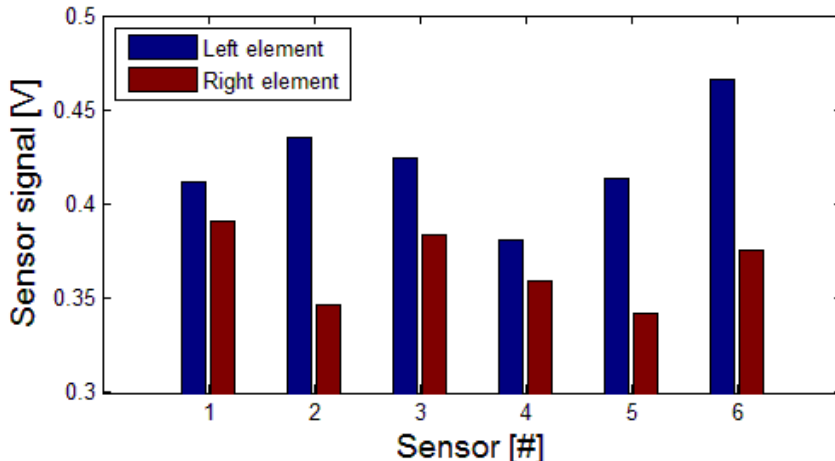


**Figure 20.** IR sensor, elements in shadow.

The mean value signal when the elements are not directly hit by the light is 0.39 V. The maximum signal is 118.2 % of the mean value signal and the minimum signal is 86.7 % of the mean value signal. The difference between the maximum and minimum signal is 26.6 % if defined according to equation 13.

Below the same test was done for the Dim sensor. This sensor sensing elements are facing in the same direction, so only one test was done.

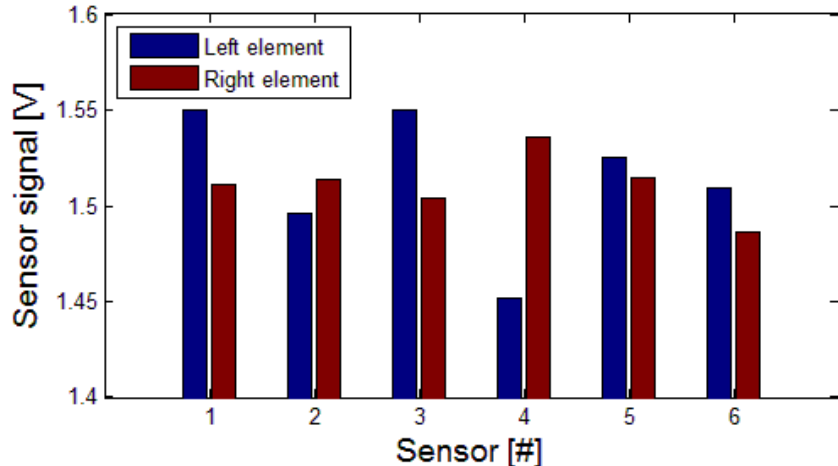


*Figure 21. Dim sensor.*

The mean value of the signal when the elements are directly hit by the light is 1.51 V. The maximum signal is 102.5 % of the mean signal, the smallest signal is 96.0 % of the mean signal. The difference between the maximum and minimum signal is 6.3 % if defined with the equation 13 above.

There are several contingencies during the tests; it is probably possible to get a result with smaller differences with better equipment. But still it is clear that the sensors output signal differs for each sensor.

### 6.3.6 Test 6 – Angular Measurement

This test was performed to evaluate the angular measurement of the two sensors. The tests were performed in a special apparatus designed by Accel. A sensor is placed under the light source. The sensor is turned  $360^\circ$  in  $10^\circ$  steps and the voltage response signals are measured. Then the sensor is elevated  $10^\circ$  and in this position turned  $360^\circ$  azimuth in  $10^\circ$  steps again. This procedure was performed for elevation steps of  $10^\circ$  until the elevation reached  $90^\circ$ . In this way the responses for changes in both elevation and azimuth are measured. In the picture below the sensor is elevated  $10^\circ$ , which corresponds to a sun elevation angle of  $80^\circ$ .

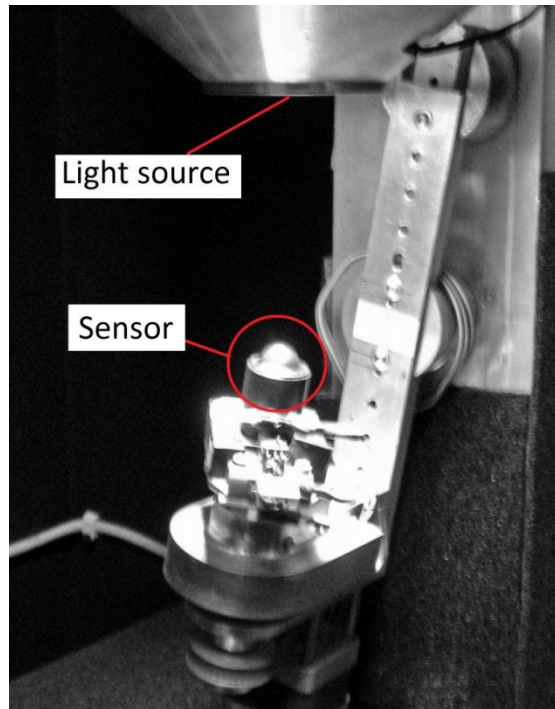


*Figure 22. Specially developed test equipment at Accel.*

In figures 23 and 24 the output signal from the sensors is displayed on the y-axis. The azimuth angle is shown on the x-axis. The red curves represent one of the sensing elements while the blue curves represent the other. The different curves are for different elevation angles. The dotted curves represent the two sensor elements for the elevation angle of  $40^\circ$  and the thin curves represent the elevation angle  $90^\circ$ .

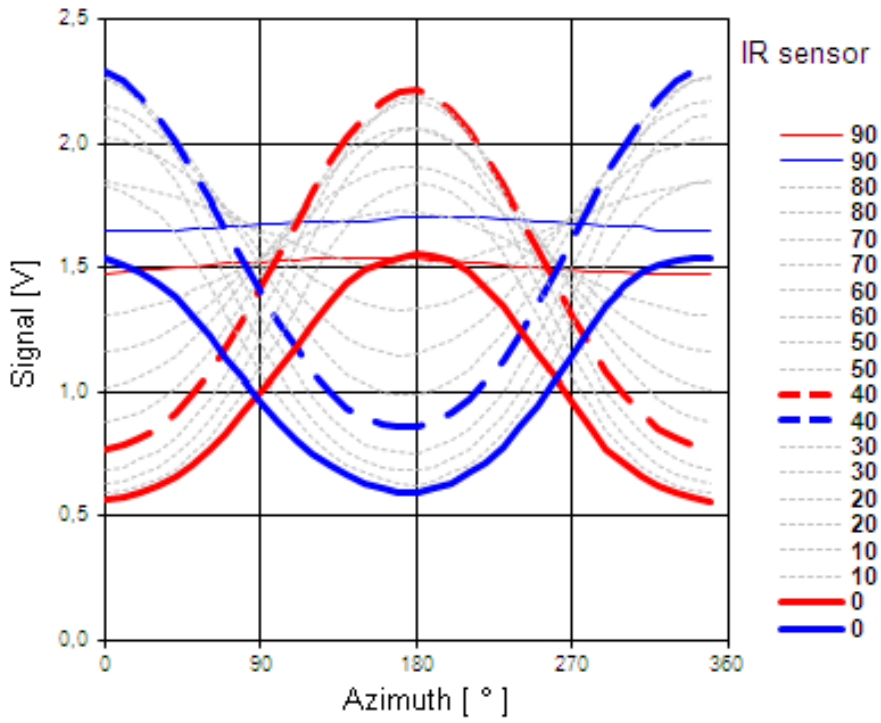


**Figure 23.** IR sensor, output signal on the y-axis and azimuth on the x-axis.

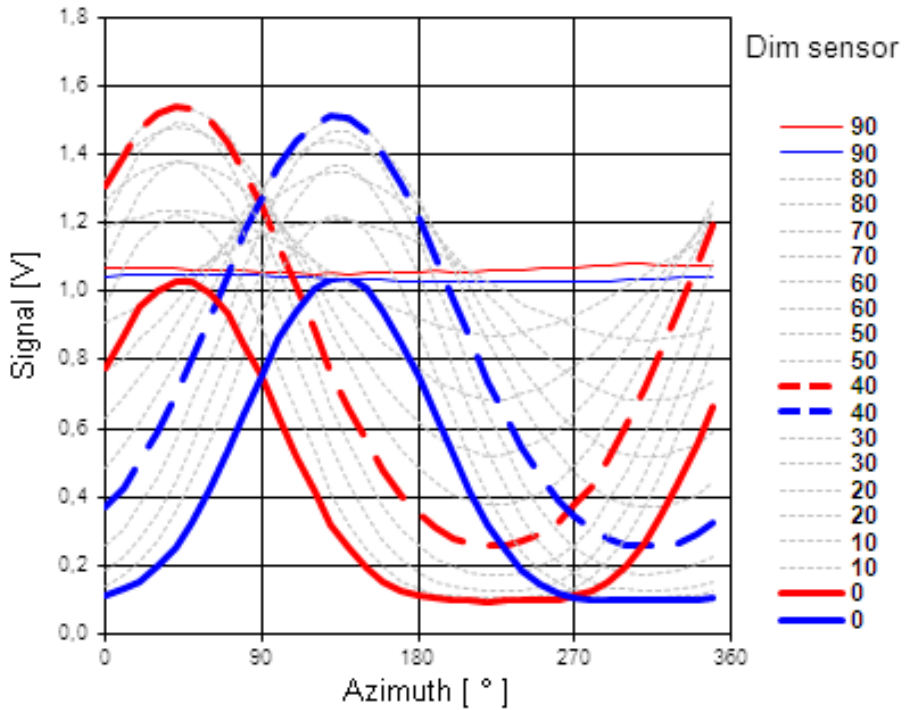


**Figure 24.** Dim sensor, output signal on the y-axis and azimuth on the x-axis.

The amplitude of the curves above represents the elevation angle. This is due to that at the lowest elevation angle one sensor is not hit by the light while the other is directly hit by the light, when the sensor has turned  $180^\circ$  azimuth the other sensor is directly hit and the other is in shadow. The azimuth angle is defined to be  $90^\circ$  in the driving direction in this case. The elevation is zero when the sun is on the horizon and  $90^\circ$  when the sun is in zenith. The almost straight lines in the middle of the figure are hence at elevation  $90^\circ$ .

Due to different techniques the two dual zone sensors have different angular response. The IR sensors response is symmetrical due to its construction with two sensor elements in different directions. The Dim sensors sensing elements are located on the same side of a flat plate separated by a divider.

In the two diagrams below the circles represent the sensor signal, the numbers outside the circle represent the azimuth angle and the blue and red lines mark the output at different elevation heights.

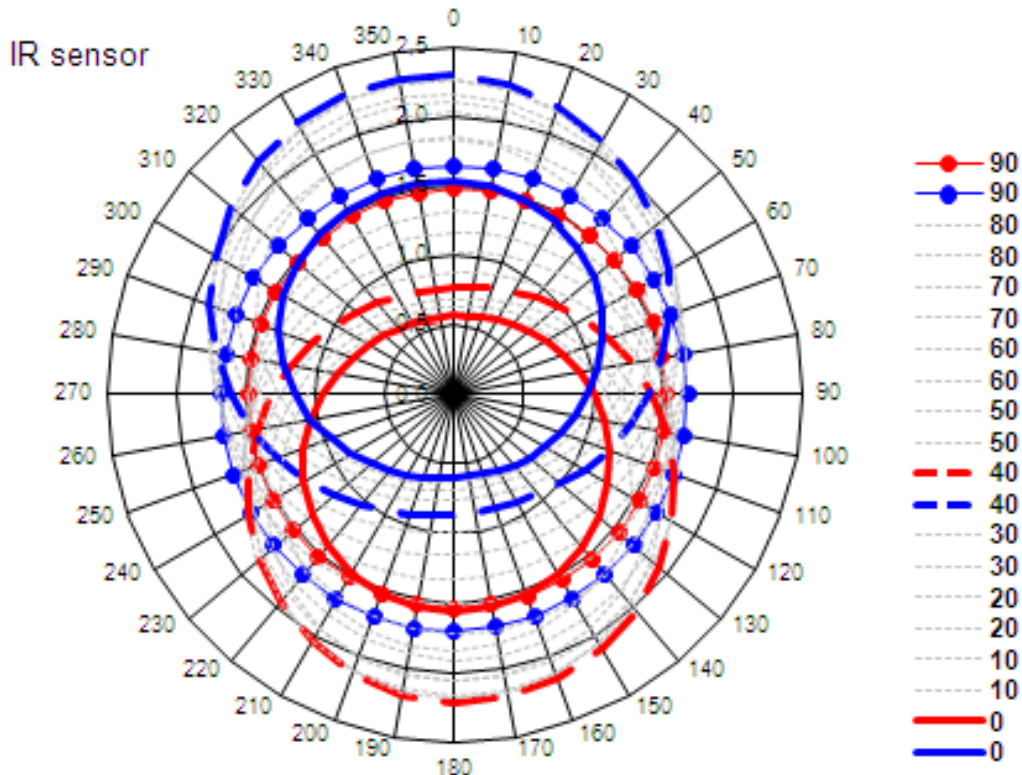


*Figure 25. Output signal, IR sensor.*

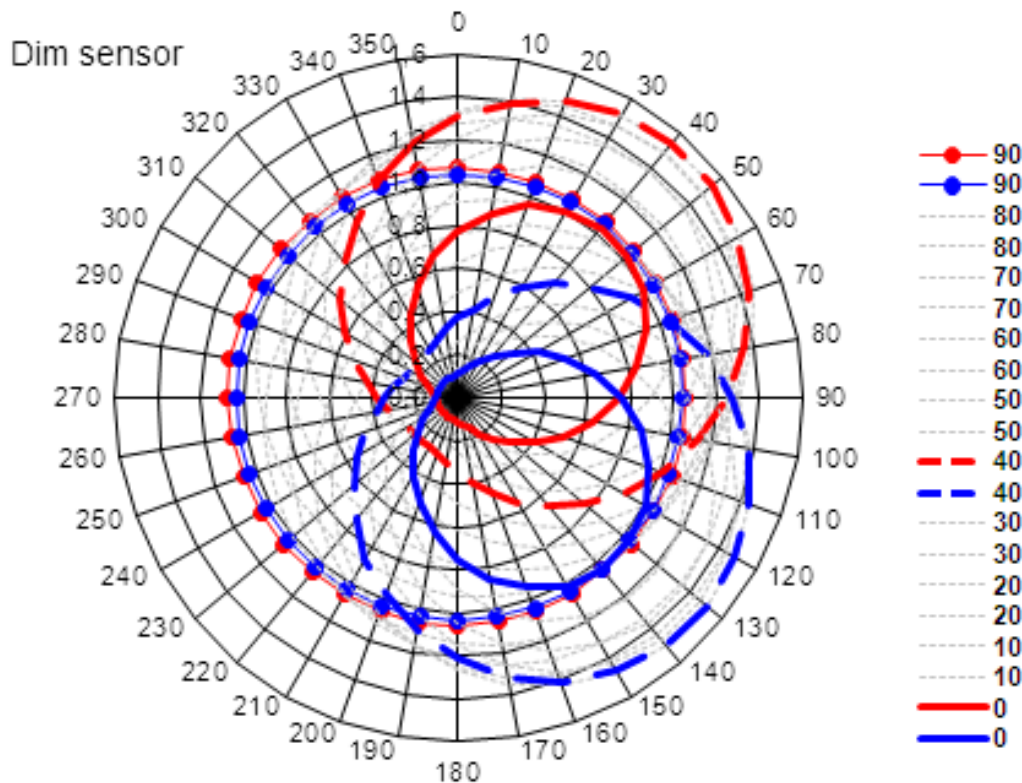


**Figure 26.** Output signal, Dim sensor.

As seen in the diagrams above the Dim sensors signal is strong when the sun hits the front and sides of the vehicle. The front of the truck is in this case at azimuth  $90^\circ$ , the azimuth is shown in the outer circle of the diagram above. The signal from the sensing element is stronger when the curve is further from the center of the circle.

For truck applications the Dim sensor should be sufficient since no sunlight comes from the back of the truck into the cabin. The IR sensors signal is stronger when the sun hits the sides of the vehicle, which is unnecessary for truck applications.

The signal in both cases is quite strong when the sun at elevation angle of  $90^\circ$ , which demonstrates the importance of the placement of the sensor. If the sun has a high elevation angle a small amount of sunlight comes in from the windshield but the sensor is still hit by the sun and sends a strong signal.

## **6.4 Conclusions**

- From the first test it is possible to conclude that the supplier of the windshield in this case presented data which could be confirmed by a simple test.
- The results from the second and third test show that it is difficult to predict the transmittance of the combination of sensor casing and windshield. Hence more tests and for each applications will be needed to get accurate results.
- The fourth test show that the transmittance of the windshield depends on the angle of the sun, however this does affect the performance of the sensor in a negative way if the sensor is placed inside the cabin.
- The fifth test concludes that the output signal of the same type of sensors varies under equal testing situations. In this test as much as 6% difference in signal between the biggest and smallest signal, this can however depend on more variables than just difference between the sensors in the batch such as inaccurate placement of the sensors.
- The sixth test shows that the design of a dual zone solar sensor has a great impact on the function of the sensor. Depending on how the sensor measures the angel of the sun the accuracy of the angular measurement will differ for different directions.



## **7 Ideas for Improvements Outside the Scope**

During the thesis other ideas for improvement of the cabin climate evolved. In this chapter, two ideas outside the scope are presented.

### **7.1 CO<sub>2</sub> Measurement**

A measurement of the concentration of CO<sub>2</sub> in the air provides a good indication of the quality of the air, the higher concentration of CO<sub>2</sub> the poorer the air quality is. It is not the CO<sub>2</sub> itself that results in poor air quality but high levels of CO<sub>2</sub> indicates high levels of contaminations caused by human activities. (Grondzic, 2007)

The concentration of CO<sub>2</sub> in the outdoor air is normally 300-400 ppm. It is said that a concentration of CO<sub>2</sub> that is under 1000 ppm is acceptable in buildings. (Folkhälsoguiden, 2003) However, humans can feel drowsy and suffer from headache due to bad air quality when the concentration of CO<sub>2</sub> is too high. Hence, in order to keep the driver alert to minimize the risk of accidents it is important to ensure a sufficient intake of fresh air into the compartment of the truck.

In the case of normal driving there is rarely a problem of bad air quality because of a good addition of fresh air. The situations when the risk is the highest of having a bad air quality in the compartment of the truck is when the fresh air flap is closed or during night time when the driver is asleep. (Fellbom, 2012) The fresh air flap can be closed due to signals from the AQS sensor detecting high concentrations of pollutants in the outdoor air and as a result the compartment air is recirculated. Often it is preferably to have a higher concentration of CO<sub>2</sub> than to risk allowing hazardous pollutants to enter from the outdoor air. However, the most interesting aspect of measuring the CO<sub>2</sub> concentration is when the driver is sleeping and the fresh air intake is minimal.

### **7.2 How to guarantee good air quality**

There are two main alternatives to guarantee a good air quality in the cabin; by forced ventilation, also called Constant Air Volume (CAV), or by measuring the concentration of CO<sub>2</sub> and other harmful gases.

When the alternative of forced ventilation is used there is a great risk of having an excessive ventilation rate or a ventilation rate that is not sufficient to maintain a good air quality in the cabin. When the cabin is ventilated more than needed the energy consumption of the climate system unit is unnecessarily high, therefore it is of great interest to keep the ventilation rate as close as possible to the optimum. As stated above it can be difficult to both maintain a good air quality and keep the energy consumption of the climate system unit as low as possible without somehow measuring the quality of the air.

One option to facilitate the control of the air quality is to implement a CO<sub>2</sub>-sensor. The CO<sub>2</sub>-sensor should be placed in such a way that it can measure the CO<sub>2</sub> concentration in the compartment air.

General Electric (GE) has a sensor designed for automotive applications. The sensor can be placed at the air outlet or anywhere inside the cabin, since CO<sub>2</sub> is mixed quickly with the air in the cabin. CO<sub>2</sub> sensors have been used for a while in buildings and the technique is well known. It is also possible to use Volatile Organic Compounds (VOC) sensors which measures the concentration of several organic gases. The VOC sensor can hence measure bad smells such as from manure on fields outside the vehicle. But according to GE it is difficult to estimate how well these sensors would work. (Olsson, 2012)

### **7.3 Maximum Ventilation Button**

It is believed that drivers does not always have the patience to wait for the cabin to heat up when the climate is cold. Then the driver might start change the temperature setting of the climate control system to ensure that the cabin is heated faster. This results in that after a while the cabin might be too hot and the driver lowers the temperature and since the reaction of the body to changes in temperature is not instantanious the cabin might be to cold after a while. To be able to avoid this situation it is possible to introduce a button that can be used to speed up the ventilation, heating or cooling to maximum. The maximum speed of the climate control will be determined by the control system and the hardware.

## 8 Results - Summary

The following questions were stated in the scope of the thesis.

- How fast and accurate does a solar sensor have to be so that it can perform as well as possible together with the other parts of the climate control system?
- What kind of solar sensors exist on the market today?
- How should the solar sensor be placed to get the best performance?
- Is it needed to perform physical tests on a solar sensor or is it possible to forecast its performance by gathering data from suppliers and calculating?

With the dimensioning parameters used in the simulations, a window area of  $1.39 \text{ m}^2$ , a supply air flow rate of  $0.05 \text{ m}^3/\text{s}$  and solar radiation intensity of  $900 \text{ W/m}^2$ , the following results were obtained. The required accuracy of the solar sensor is about  $\pm 6 \text{ W}$  or  $\pm 4.5 \text{ W/m}^2$ . The time constant was calculated to be 1.26 and is therefore recommended to be between one and two seconds. The corresponding recommended rise time is about two seconds, calculated to be 1.8 seconds.

Several techniques are used to measure the impact of sunlight in vehicles. All of the sensors examined in the benchmark had a time constant smaller than the one derived from the simulations. Hence, the time constraint of the solar sensor is of minor importance when comparing the manufacturers since most of fulfill the required time. However, it was not possible to compare the accuracy of the solar sensors in the benchmark due to insufficient information from the suppliers. Some sensors can be combined with other functions like a twilight sensor. Most of the sensors are customized products, which imply that sensors can be redesigned to fit the purpose of the user as best as possible.

It is recommended to use a sensor that can measure the elevation, the azimuth and the intensity of the sunlight. In addition it is recommended to design a control system which can calculate the sun load entering the cabin with help from these parameters as can be seen in chapter 5.

The sensor should be placed on the inside of the windscreen to be able to measure the sunlight intensity transmitted through the glass as shown in test 4 in chapter 8.

Tests, before final tune in of the control system, are needed for each combination model of sensor and vehicle to get accurate results. This is due to that different combinations of windshield glass, sensor casings and sensor designs will result in different sensor outputs for different wavelengths. Also the reflectance of the surface on which the sensor is placed will impact the measurement of the sensor. All these factors are difficult to take into account while calculating, it is therefore of importance to perform physical tests. However, it might be possible to try to predict the performance of the sensor by calculation and tuning of the control system.



# **9 Discussion**

In the following chapter the results gained are discussed.

## **9.1 Time Constraints and Accuracy**

To be able to simulate the energy balance of a cabin a model designed for energy balances in buildings was used. The model was modified to be used to simulate a truck cabin, data concerning the geometry of the cabin and different heat transfer constants of the walls of the cabin were measured and approximated from various tables.

At the first it was thought that the simulations of the heat balance in the truck performed in the thesis would lay as a ground for further more complex simulations performed by Volvo Group. However, the simulations performed proved to provide reasonable values for the accuracy and the time constraint of a possible future solar sensor. Hence, the simulations performed in this thesis shows that there may not be a need to investigate a more complex and certainly more expensive model developed for truck or vehicle aspects. As a matter of fact it could be better to use a heat balance model developed for buildings than to use a similar model that is developed for cars. This is due to the geometrical aspects of the truck cabin, as the cabin is more or less a box. The geometrical aspects of a building are rather similar to those of a truck cabin even though a building of course is much larger than the cabin of a truck. Hence, it is easier to adapt a model that originally was developed for a building than to try to adapt a model designed for cars.

It would be a good idea for the Volvo Group to acquire data of the heat transfer coefficients of the materials used in the cabin. If simulations of the heat balance would be performed again this would provide even more strength to the results if the actual heat transfer coefficients of the material used in the trucks would be used instead of general values of similar material that were used in these simulations. However, to get an appreciation of the accuracy and the time constant of a solar sensor the values derived in this thesis are valid to use due to that the heat transfer coefficient does not affect the results of the heat balance to a great extent.

If the Volvo Group would look into investing in the model that were used in the thesis or in a similar one it would be possible to make further simulations in order to evaluate different driving circumstances. The simulation was based on the parameters of a still standing truck it could be interesting to evaluate how different driving circumstances would impact the result. Other driving circumstances were not evaluated in this thesis since it was chosen to look at the worst case scenario, which is when the truck is standing still.

In the beginning of the simulations questions were raised concerning that the simulation would be too general and that it might not provide results usable at all. However, since the results were validated by both the feature leader of climate and the software producer the generality of the simulations was observed in a different light. As the Volvo Group has several different truck brands within the group the results from the model can be used for all these brands of trucks. Hence, for example there is no need to perform two simulations to investigate the heat balance of a Volvo truck and a Renault truck, it is sufficient to perform one simulation for both.

In the simulations it was stated that the feedforward system should manage to detect and reduce the impact off a sun load giving rise to an increase of one degree Celsius or more of the cabin air. It could be interesting for the Volvo Group to investigate up till which temperature increase the feedforward system should be able to detect and reduce the impact the entering load if a solar sensor would be used. The investigation could also include determining when the feedback system should be activated to offset the load.

## 9.2 Benchmark

The benchmark was performed in order to gain knowledge about the sensors available on the market and to make a comparison between these sensors to find the sensor most suitable for the purpose. Several sensor manufacturers were contacted and asked to take part in the benchmark. Some of the manufacturers were interested in participating and provided information about their sensors and some suppliers were not interested in participating.

The data sheets provided by those manufacturers that chose to take part in the benchmark were evaluated and the functional parameters of the different sensors were compared. However, the manufacturers chose to put diverse functional parameters in their product specifications mainly due to that several functional parameters of the sensors are custom made and can therefore not be published in data sheets. Another reason can be due to marketing reasons, the manufacturer may not want to present parameters of the sensor that do not have a high standard. This lack of uniformity of stated parameters in the data sheets made it difficult to perform a thorough comparison of the sensors.

However, it was seen that all of the solar sensors examined had shorter time constants than the time constant derived in the simulations. This implies that the time constant will not be the critical parameter when choosing a solar sensor. Hence, Volvo Group should not focus on improving the time constant of a future solar sensor since it is already more than fulfilled by the sensors already existing on the market.

The accuracy parameter is one of the most critical parameters when choosing a solar sensor, however the accuracy parameter is in most cases custom designed and is therefore not presented in general sensor data sheets. No comparison of the accuracy of the sensors was performed due to this absence of data. Volvo Group is recommended to collaborate with some of the manufacturers in order to evaluate the accuracy of a solar sensor. Volvo Group is recommended to collaborate with Accel and GE Measurement & Control, since these two manufacturers were easy to collaborate with.

It is recommended to the Volvo Group to state the main required parameters of a possible future solar sensor in order to facilitate a future more detailed benchmark. However, since several of the parameters of importance are custom made it would be difficult for Volvo Group to gather the information necessary without entering further discussions and cooperation with the manufacturers.

## **9.3 Placement**

Several factors must be taken into consideration when determining the placement of a sensor. The placement of the sensor is dependent on mainly its functionality, meaning in which way the sensor measures the incoming sun load intensity, its design and how sensitive it is to shielding objects such as the roof. Other important factors when deciding the position of the sensor are the esthetical appearance of the sensor and the possibility of connecting electrical wires. It is important to perform tests of the placement of the sensor due to that the surroundings of the sensor influence greatly on the performance of the sensor. For example the senior director Arvydas Maldžiūnas at Accel explained how the reflectivity of the surface on which the sensor is mounted affects the performance of the sensor. Hence, if the dashboard is available in dark and light colors the sensor should be evaluated with each dashboard color before designing the control system.

In chapter 5 the importance of the placement of the sensor was highlighted by an example explaining the difference by measured sun load and actual entering sun load. Hence, it is of great importance to carefully evaluate the exact position and inclination of the sensor before designing the control system.

It was also seen that the energy transmitted in to the cabin was greatly depending on the transmittance of the windshield and the angle from which the sunlight hits the truck. If an external solar sensor would be used the impact of the windshield must be compensated for in the control system. In addition an external solar sensor would quickly be worn out and particles might cover the sensing area of the sensor and by that reduce the sensors ability to sense. Therefore, it is recommended to place the sensor inside of the cabin and it is also recommended to avoid assigning too much time and resources on the investigation of an external solar sensor.

## **9.4 The Tests**

The tests were performed in cooperation with the sensor manufacturer Accel in Lithuania during a limited time. The tests were performed in order to examine the influence of the windshield glass on the performance of the sensor. Due to the time limit of the tests there were some factors limiting the precision of the tests. However, the tests performed do demonstrate the importance of the usage of the windshield glass while evaluating the performance of the sensor.

The output signal of the sensor when a windshield was placed between the light source and the sensor was about 35 % to 37 % of the full output signal, this can be seen in chapter 8. These results emphasize the importance of testing the performance of the sensor with the windshield glass before developing the control system. This is due to that the windshield might not transmit so much energy in certain wavelengths, which can make the transfer function delivered by the supplier inaccurate.



## **10 Recommendations**

A solar sensor should be used to forecast an increase in temperature in the cabin. Hence, it is recommended to choose a solar sensor which can sense both elevation and azimuth angle and the intensity of the sunlight.

It is recommended that a solar sensor with a time constant lower than two seconds is used. The accuracy of the sensor should be within  $\pm 6$  W and  $\pm 4.5$  W/m<sup>2</sup>. The accuracy or rather the inaccuracy in this case is the maximum error allowed to be able to control the temperature within  $\pm 1$  °C in the cabin. All of the solar sensors examined in the benchmark are more than fulfilling the time constant requirement. It is therefore not recommended to engage conversations with the manufacturer in order to lower the time constants of the sensors available. Some suppliers can deliver a combined sun and twilight sensor, if a twilight sensor is to be used, it can be a good option.

It is recommended that Volvo Group test their sensors in the environment of which they are supposed to be used. The solar sensor should be placed inside the cabin and the exact placement should be well thought through. The control system must be designed in a way so that with help from the elevation and azimuth angles it can calculate the window area projected on a plane perpendicular to the sunlight. In this way the total amount of energy from the sun transmitted to the cabin can be calculated and a temperature increase forecasted.

If the choice stands between choosing a sensor with elements facing opposite sides or a sensor with elements facing the same side separated by a divider, then the sensor with the divider is preferable. It is also recommended to have in mind that the output signal varies to some extent for the same kind of sensor.

For future improvements for the cabin comfort it is also recommended continue the investigation of a CO<sub>2</sub> sensor. Using a CO<sub>2</sub> sensor facilitate to keep the air healthy air and optimize energy use.



## Works Cited

- Agilent Technologies.** 2012. *Practical Temperature Measurements*. USA : Agilent Technologies, 2012.
- Alciatore, David G. and Histand, Michael B.** 2007. *Introduction to mechatronics and measurement systems*. 3rd. New York : McGraw Hill, 2007.
- Coers, Mardi, Chris Gardner, Lisa Higgins, and Cynthia Raybourn.** 2001. *Benchmarking: A Guide for Your Journey to Best-Practice Processes*. s.l. : APQC, 2001. Online version available at: <http://common.books24x7.com.proxy.lib.chalmers.se/toc.aspx?bookid=8743>.
- Daly, Steven.** 2006. *Automotive air-conditioning and climate control systems*. s.l. : Elsevier Ltd, 2006. ISBN 978-0-7506-6955-9.
- Fellbom, Henrik.** 2012. *Volvo GTT Consultant*. Spring 2012.
- Folkhälsoguiden.** 2003. *Hälsobesvär av inomhusmiljön*. Stockholm : Arbets och Miljömedicin, 2003. <http://www.folkhalsoguiden.se/upload/Milj%C3%B6/Milj%C3%84B6%20infomaterial/Faktatext%20om%20inomhusmilj%C3%84B6%20inklusive%20referenser.pdf>.
- Fraden, J.** 2004. *Handbook of Modern Sensors: Physics, Designs and Applications*. New York : Springer Science + Business Media, 2004.
- Grondzic, Walter.** 2007. *Air Conditioning System Design Manual*. 2007. Second Edition.
- Gruber, Mattias.** 2012. *Demand-based control of indoor climate in office buildings - Design of central and local feed-forward control systems for high comfort, low energy use and low peak power*. Gothenburg : Chalmers University of Technology, Building Services Engineering, 2012.
- Incropera, et al.** 2007. *Fundamentals of Heat and Mass Transfer*. USA : John Wiley & Sons, Inc., 2007.
- Lennartson, Bengt.** 2002. *Reglerteknikens grunder*. Lund : Studentlitteratur, 2002. 91-44-02416-9.
- Mårdberg, Björn.** 2012. VTEC. Spring 2012.
- Newport.** *ORIEL PRODUCT TRAINING - Solar Simulation*. Stratford : Newport. [www.newport.com/oriel](http://www.newport.com/oriel).
- Ocean Optics.** *LS-1 Series Tungsten Halogen Light Sources*. More info: [www.oceanoptics.com/products/ls1.asp](http://www.oceanoptics.com/products/ls1.asp).
- . 2006. *USB4000 Fiber Optic Spectrometer - Installation and Operation Manual*. FL, USA : Ocean Optics, Inc., 2006. Document Number 211-00000-000-02-1006.
- Olsson, Anderas.** 2012. *GE Measurement & Sensing*. May 23, 2012.
- Petersson, Bengt-Åke.** 2009. *Tillämpad Byggnadsfysik*. s.l. : Studentlitterature AB, 2009. 9144058179.
- SMHI.** 2007. Solstrålning. [Online] April 2007. [Cited: May 3, 2012.] [http://www.smhi.se/polopoly\\_fs/1.6403!faktablad\\_solstralning%5B1%5D.pdf](http://www.smhi.se/polopoly_fs/1.6403!faktablad_solstralning%5B1%5D.pdf).
- Stapenhurst, Tim.** 2009. *Benchmarking Book - A How-to-Guide to Best Practice for Managers and Practitioners*. s.l. : Elsevier, 2009. Online version available at: [http://www.knovel.com.proxy.lib.chalmers.se/web/portal/browse/display?\\_EXT\\_KNOVEL\\_DISPLAY\\_bookid=2526&VerticalID=0](http://www.knovel.com.proxy.lib.chalmers.se/web/portal/browse/display?_EXT_KNOVEL_DISPLAY_bookid=2526&VerticalID=0).
- TECHMATION.** Application Manual - Chap 10. Feedforward Plus Feedback. [Online] [Cited: Juli 15, 2012.] <http://protuner.com/>.
- Tille, Thomas.** 2010. *Automotive suitability of air quality gas sensors*. s.l. : Elsevier, 2010.
- Wilson, Jon S.** 2005. *Sensor Technology - Handbook*. Burlington : Elsevier, 2005.
- Volvo GTT.** 2. *Inhouse document*. 2.
- . 1. *Inhouse document*. 1.
- . 3. *Inhouse document*. 3.
- . 4. *Inhouse document*. 4.

## Figure Sources

- Figure 1:* Inspired by **Wilson, Jon S. 2005.** *Sensor Technology - Handbook.* Burlington : Elsevier, 2005.
- Figure 2:* Inspired by **Lennartson, Bengt. 2002.** *Reglerteknikens grunder.* Lund : Studentlitteratur, 2002. 91-44-02416-9.
- Figure 3:* **Volvo GTT.** *Inhouse document 5.*
- Figure 10:* **Ocean Optics 2006.** *USB4000 Fiber Optic Spectrometer - Installation and Operation Manual.* FL, USA : Ocean Optics, Inc., 2006. Document Number 211-00000-000-02-1006.
- Figure 11:* **Newport.** *ORIEL PRODUCT TRAINING - Solar Simulation.* Stratford : Newport. [www.newport.com/oriel](http://www.newport.com/oriel).
- Figure C 1:* Inspired by **Alciatore, David G. and Histan, Michael B. 2007.** *Introduction to mechatronics and measurement systems.* 3rd. New York : McGraw Hill, 2007.
- Figure C 2:* **Tille, Thomas. 2010.** *Automotive suitability of air quality gas sensors.* s.l. : Elsevier, 2010
- Figure C 3:* **Tille, Thomas. 2010.** *Automotive suitability of air quality gas sensors.* s.l. : Elsevier, 2010

## Appendix A – Resistance Sensor, Wheatstone Bridge and Transfer Function.

A basic setup for a resistive sensor called a voltage divider is shown below.

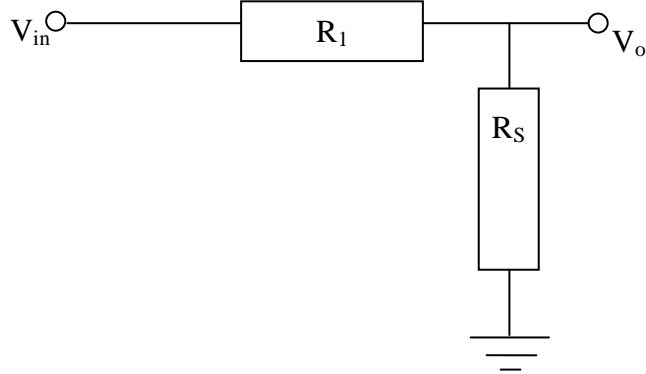


Figure A 1: Voltage Divider.

According to Ohm's law and Kirchoff's rules:

$$V_{out} = \frac{R_s}{R_1 + R_s} V_{in}$$

If  $R_1 \gg R_s$  then the equation can be simplified to:

$$V_{out} = \frac{R_s}{R_1} V_{in}$$

As can be seen when the sensing resistance  $R_s$  varies also  $V_{out}$  varies according to the formula above. Similar setups and equations are used also for capacitive and inductive sensors, hence the capacitance or the inductance varies instead of the resistance. (Wilson, 2005)

### *Wheatstone Bridge*

An improvement of the simple voltage divider shown in the figure above is the so called Wheatstone bridge. The Wheatstone bridge consists of the voltage divider shown and two additional fixed resistors. The purpose of the two fixed resistors is to provide a reference voltage that equals the sense voltage at a specific value of the resistance of the sense resistor, the sense resistance is the resistance that varies with the property that should be measured. Then the difference in the voltages from the reference and the sensor voltage divider is measured. The output from the Wheatstone bridge is hence the difference in voltage. This signal is easier to amplify than in the case of a simple voltage divider since a simple voltage divider got a bigger offset voltage. The use of reference voltage also eliminates errors due to variations in the resistors that should be constant. (Wilson, 2005)

### *Transfer function*

The transfer function is a mathematical function or a graph showing the true variation of the output signal with regards to the input signal, this curve is sometimes the same as the calibration curve. (Wilson, 2005)

The transfer function provides the dependence between the electrical signal  $S$  and the stimulus  $s$ :

$$S = f(s)$$

This function can be either linear or nonlinear (e.g., exponential, logarithmic or power function). In many cases, the transfer function is unidimensional, hence the output is dependent on one input stimulus. This is represented by the following equation

$$S = a + bs$$

Where  $a$  is the intercept (i.e the output signal at zero input stimulus) and  $b$  is the slope, sometimes called the *sensitivity of the function*. The electrical signal  $S$  is one of the output characteristics, this may be amplitude, frequency or phase depending on the properties of the sensor.

The transfer function may also be multidimensional, hence the output signal is dependent on more than one input stimuli.

## Appendix B – Sensor Parameters

There are several parameters that are important when choosing a sensor; some of these are listed below.

### *Span (Full-Scale Input)*

The *span* is a dynamical range of stimuli which may be converted by a sensor. The span represents the highest possible value of stimuli that may be applied to the sensor without causing unacceptably large inaccuracy. (Fraden, 2004)

### *Full-Scale Output*

The *full-scale output* is the difference between the output signal at maximum input stimuli and the output signal at minimum input stimuli. This range must include all possible deviations from the ideal transfer function. (Fraden, 2004)

### *Sensitivity*

The sensitivity shows the relationship between input and output signal, often it is described by the ratio between input and output signal. It can thus be the derivative with respect to the input signal of the transfer function. A typical unit is volt/kelvin if temperature is measured. (Wilson, 2005)

### *Accuracy*

*Accuracy*, or better stated *inaccuracy*, is often defined as the maximum error between actual and ideal output signal. (Wilson, 2005) The inaccuracy can be computed by the difference between the value that is computed from the output voltage and the input stimuli. For example, a linear temperature sensor ideally should generate 1 mV per 1 °C. However, the sensor may give an output of S=10.5 for an increase of the input stimuli by 10 °C which implies that the sensor has an inaccuracy of 0.5 °C over a 10 °C span. (Fraden, 2004)

Due to material errors, design errors and other limitations it is possible that one single sensor can have different transfer functions when tested under identical conditions. However, each time the sensor is tested its output signal should be within the limits of a specified accuracy. These limits differ from the ideal transfer function by  $\pm\Delta$  and the real transfer function deviate  $\pm\delta$  from the ideal transfer function, which implies that  $\delta \leq \Delta$ . The accuracy limits are in most cases used to determine the worst case scenario. (Fraden, 2004)

In order to make the accuracy limits narrower they are established not around the ideal transfer function but around the calibration curve (i.e. the real transfer function). By making the limits narrower it allows the sensor to sense more accurately, but often in trade for a higher cost. (Fraden, 2004)

### *Calibration*

When a sensor is calibrated its individual transfer function is determined, or more precise the unknown variables of the overall transfer function is determined. The overall transfer function includes the sensor, the interface circuit and the A/D converter. The mathematical equation should be known before calibration (i.e. if it is for example a linear or exponential function). If

the required system accuracy is narrower than the tolerances of the sensor and the interface, a calibration is needed. For a linear line a two-point calibration is needed, as two points are needed to define a straight line. For a nonlinear transfer function several calibration points may be needed. (Fraden, 2004)

When a sensor is calibrated in the factory the *calibration error* is the allowed deviation from the transfer function. The calibration error is a shift in accuracy by a constant for each stimulus point, hence the constant may not be the same over a range of stimulus. (Fraden, 2004)

#### *Hysteresis*

An error for a specific input stimulus is called a *hysteresis error*, a sensor with hysteresis does not return to the same output value for a certain input stimuli when the input stimulus is cycled up or down. (Wilson, 2005) A typical cause for hysteresis can be structural changes in the material or friction. (Fraden, 2004)

#### *Nonlinearity*

The maximum deviation of a real transfer function from the approximation straight line is called the *nonlinearity* error. This error is specified for those transfer functions that may be approximated with a straight line. (Fraden, 2004)

The error can be expressed in several ways; the way that is most profitable for the supplier is often used in the technical sheets provided by the supplier. (Wilson, 2005) Hence, when defining the nonlinearity error it is important to state what sort of line that the nonlinearity is referring to. There are several ways to classify the approximation straight line. One way is to use the terminal points, which are the two output values for the beginning and the end of the stimuli range, and draw a straight line in between. For this classification the nonlinearity errors are small near the terminal points. Another way is to use the independent linearity, also called “best straight line”, which is the line between two parallel lines that are enclosing all possible output values of the real transfer function. (Fraden, 2004)

#### *Saturation*

Although a sensor is considered to be linear it does have operating limits, at some input stimulus at the end of the span the output signal will no longer be accurate enough. This is called the *saturation* of the sensor. (Fraden, 2004)

#### *Repeatability*

A *repeatability* error occurs when the output signals differ from two identical input stimuli at identical operating conditions. The cause may be material plasticity, thermal noise and so forth. (Fraden, 2004)

#### *Bandwidth*

All sensors have a response time and a decay time, that is the time to respond to input changes and the time to reset to original value respectively. These two correspond to the upper and the lower cutoff frequency, the bandwidth is the range between those two frequencies. (Wilson, 2005)

### *Dead band*

The *dead band* is an interval of input stimuli where the sensor is insensitive and the output of the sensor may stay at a certain level, often at zero, over the entire dead band interval. (Fraden, 2004)

### *Resolution*

Sometimes the output signal from a sensor may be changed in small steps instead of a continuous change, this is due to the *resolution* of the sensor. Hence the resolution is the minimum detectable fluctuations of the incoming stimuli. The resolution may differ over the range of the input stimuli. (Fraden, 2004)

### *Output impedance*

The impedance of a circuit is the opposition that the circuit composes when a voltage is applied. To get a better knowledge about the interface between the sensor and the electronic circuit it is important to know the *output impedance* of the sensor. The impedance should be represented in complex form as it may have both active and reactive components. (Fraden, 2004)

### *Dynamic Characteristics*

The *dynamic characteristic* of a sensor is a time dependent delay factor caused by the fact that the sensor cannot always respond instantaneous. Also the control system, of which the sensor is a part, can have dynamic characteristics. At worst these delays of the true value can cause oscillations in the system. (Fraden, 2004)

The *warm-up time* of a sensor describes the time that it takes from that an electric current is applied until the sensor until the sensor produces an output signal that is within acceptable accuracy limits. (Fraden, 2004)

A way to measure the response time for a sensor is by the *time constant* which is the time that it takes for a certain sensor to reach 63% of the maximum or the steady-state level for a step stimulus. This time constant is a measure of the inertia of the sensor and is denoted  $\tau$ . The time constant is the product of the electrical resistance R and capacitance C; (Fraden, 2004)

$$\tau = C * R$$

### *Noise*

All sensors produce a background noise in addition to the desired output signal. In some cases the noise signal disturbs the performance of the sensor. The noise is often distributed over the frequency spectrum. (Wilson, 2005)



## Appendix C – Some Basic Types of Sensors

In this appendix some types of sensors and techniques are presented.

### Temperature Sensors

Several technologies can be used to measure properties of the surrounding environment of the sensor, in the following section some of them are presented.

#### Thermistors

A thermistor is a temperature sensitive resistor. Thermistors often consist of two or three metal oxides sintered in a ceramic base, forming a semiconductor. The resistivity of semiconductors change more when introduced to a temperature change than other resistors do. The temperature coefficient for a thermistor can be either positive, Positive Temperature Coefficient (PTC), or negative, Negative Temperature Coefficient (NTC). The resistance increases with temperature for a PTC thermistor and decreases for a NTC thermistor. The change of resistance is larger in NTC thermistors, which makes a sensor with NTC more sensitive, it is also easier to produce the NTC devices smaller and with faster thermal response than the PTC devices. (Wilson, 2005) PTC thermistors can be produced using conductive polymers, making use of the phase change of the polymer. When temperature increases the resistance increases fast, so this kind of thermistors can be of good use for example in protection of high temperatures. (Wilson, 2005)

The resistance in a thermistor varies exponentially, following the relationship below.

$$R = R_0 e^{[\beta(\frac{1}{T} - \frac{1}{T_0})]}$$

Where  $R$  is the resistance and  $R_0$  is the resistance at the reference temperature.  $T$  is the measured temperature,  $T_0$  is the reference temperature and  $\beta$  is the calibration constant called the “characteristic temperature” of the material. (Alciatore, o.a., 2007)

Thermistors have better accuracy than a resistive temperature device, which is explained below, but also a smaller operating temperature range. (Alciatore, o.a., 2007)

#### Resistive Temperature Device

A Resistive Temperature Device (RTD) has just as the thermistor a resistor as the sensing element. The resistor of the RTD usually consists of a metal wire coil with a ceramic or glass core inside a casing. (Alciatore, o.a., 2007) Platinum is often used since it can withstand high temperatures and maintain stability, and since it is a noble metal it is not easily contaminated. (Agilent Technologies, 2012) The typical operating temperature range for platinum RTD is -220°C to 750°C. (Alciatore, o.a., 2007)

The resistance of a RTD changes as follows:

$$R = R_0(1 + \alpha(T - T_0))$$

Were  $R$  is the resistance and  $R_0$  is the resistance at the reference temperature (often  $0^\circ\text{C}$ ).  $T$  is the measured temperature,  $T_0$  is the reference temperature and  $\alpha$  is the calibration constant. (Alciatore, o.a., 2007)

## Thermocouples

A thermocouple consists of two metals or alloys joined together in two ends. A thermocouple has a “hot” junction and a “cold” reference junction. The hot junction is where the temperature is measured. When the two junctions are exposed to different temperatures a current, proportional to the temperature will flow through the wires. (Wilson, 2005) If the circuit is cut off, the voltage potential can be measured. (Agilent Technologies, 2012)

The fact that a voltage potential is formed is a phenomenon called the Seebeck effect. The picture below shows two metals, A and B and the two junctions of the metals. There are different temperatures  $T_1$  and  $T_2$  at the junctions, hence the Seebeck effect is valid and a voltage can be measured. (Alciatore, o.a., 2007)

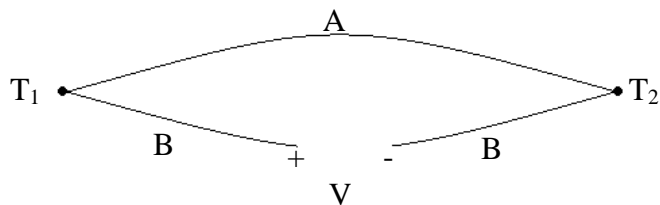


*Figure C 1: Thermocouple*

The voltage is directly proportional to the temperature difference, according to:

$$V = \alpha(T_1 - T_2)$$

Were  $\alpha$  is the Seebeck coefficient. (Alciatore, o.a., 2007)

Thermocouples can handle much higher temperatures than for example a RTD since no sensing elements are used. (Wilson, 2005)

## Silicon sensors

One type of silicon sensor is the Integrated Circuit (IC) sensor that is composed of semiconductors just like the thermistor. The increase in resistance of a silicon sensor is nearly linear at low temperatures, with a positive temperature coefficient. (Wilson, 2005)

IC sensors exist with both voltage and current output variants and the linear output signals typically can be in the form  $1\mu\text{A}/\text{K}$  or  $10\mu\text{A}/\text{K}$ . Some IC sensors have a microprocessor and their output is digital, hence there is no need for A/D conversion. These IC sensors have the same disadvantages as the thermistors, they have a limited temperature range and they need an external power source. (Agilent Technologies, 2012)

## Infrared pyrometer

All objects emit infrared radiation directly correlated to the temperature of the object. The infrared (IR) sensors measure the infrared radiation and convert the stimulus to voltage. (Wilson, 2005)

There are several factors contributing to the accuracy of measuring with IR sensors:

- Reflectivity, measure of how big part of the radiation that is reflected compared to the radiation that falls on to the surface of an object.
- Transmittance, measure of how big part of the incident radiation that passes through the object at a specific wavelength.
- Emissivity, the ratio of how much radiation that is emitted from the objects surface compared with a perfect object (black body) at the same temperature. (Wilson, 2005)

## Humidity Sensors

The humidity sensors measures the water content of the air, this measurement can be done in several different ways some of them are described below.

The *absolute humidity* is the density of the water vapor in grams per cubic meter. Because of that the absolute humidity is dependent on the atmospheric pressure the absolute humidity it is not often used in practice. (Fraden, 2004)

The *relative humidity* is the ratio of the partial pressure of water vapor and the pressure of the saturated water vapor at a given temperature. (Fraden, 2004)

$$RH = 100 * \frac{P_w}{P_s}$$

Where  $P_w$  is the pressure of the water vapor and  $P_s$  is the pressure of the saturated water vapor. In the given equation the relative humidity is given in percentage. In other words the relative humidity describes how much water the air contains compared to how much it can contain at maximum for a given temperature. A rule of thumb is to have a relative humidity of 50 % at normal room temperature (20 °C – 25 °C). (Fraden, 2004)

The *dew point temperature* is the temperature to which the humid air needs to be isobaric cooled to induce fog on the windshield. At the dew point the relative humidity of the air is 100 %, hence the air is saturated. A chilled mirror is often used to measure the dew point temperature, however below 0°C this measurement technique becomes uncertain as the moisture in the air at one point will freeze and form a crystal lattice on the surface of the mirror. However the moisture in the air can remain in a liquid phase below 0 °C depending of the rate of convection and contaminations and so forth. (Fraden, 2004)

To measure humidity, moisture and dew temperature sensors that are conductive, capacitive, optical or oscillating can be used. (Fraden, 2004)

## **Capacitive Humidity Sensor**

The moisture content in the air changes its electrical permeability therefore a capacitive sensor can be used to measure the relative humidity of the air. The permeability of the air changes according to:

$$\kappa = 1 + \frac{211}{T} * \left( P + \frac{48 P_s}{T} * H \right) * 10^{-6}$$

Where  $T$  is the absolute temperature (K),  $P$  is the pressure of the moist air (mm Hg),  $P_s$  is the pressure of the saturated water vapor at temperature  $T$  (mm Hg),  $H$  is the relative humidity (%). According to the equations above and below the capacitance is proportional to the relative humidity of the air. (Fraden, 2004)

$$C = \frac{\kappa * A}{d}$$

Instead of using air an isolator can be inserted in the space between the plates of the capacitor, the dielectric constant of the insulator needs to change considerably when it is in contact with humid air to be able to give a measurement of the relative humidity of the air. In this case the capacitance is approximately proportional to the relative humidity. (Fraden, 2004)

## **Electrical Conductivity Sensor**

A conductive hygrometric sensor contains a nonmetal conductive top layer. The top layer is made of a material that has a relatively low resistivity that changes drastically when imposed to humidity. Underneath the top hygrometric layer are two interdigitized electrodes, when the top layer absorbs water molecules the resistivity between two interdigitized electrodes changes and this change can be measured with an electronic circuit. (Fraden, 2004)

## **Thermal Conductivity Sensor**

A thermistor based sensor can be used to measure the humidity from the thermal conductivity of the gas. The sensor contains two thermistors; one exposed to the outside gas and the other hermetically sealed in dry air. The two thermistors are connected in a bridge and due to the passage of electric current the thermistors heats up. To establish a zero reference point the bridge is balanced in dry air and when the absolute humidity increases from zero the output voltage of the bridge increases. (Fraden, 2004)

## **Solar sensors**

Absorption of photons can result in two different responses, quantum or thermal. A quantum response converts the energy of the incoming photon directly to an electron in the conductive layer of the semi-conductor. While the quantum response detectors operate in the ultraviolet to mid-infrared spectrum the thermal response detectors operate from mid-infrared to far-infrared spectrum. (Fraden, 2004)

The detectors giving a quantum response has the best performance for detecting incoming optical radiation. If the energy of the photon is high enough it will be absorbed by the detector and the

energy released from the photon excites an electron from the valence band to move to the conductive band. After being excited the electron is free to move in the conductive band. A p-n junction in a p-n photodiode creates a step which results in a direction for the created current to take. Photovoltaic and photoconductive are examples of photodiodes. (Fraden, 2004)

The thermal detectors absorb infrared radiation and measure the temperature increase with a thermometer. (Fraden, 2004)

## **Chemical sensors**

Chemical sensors are used to detect chemical compounds and their concentration. The technique used for detecting chemicals is different depending on the properties of the chemical that should be detected. One property that can be used to distinguish between different molecules is the vibration or rotation modes, these modes are often unique to specific molecules. Since these molecules can absorb or emit a photon, getting excited or relaxed, it is possible to use infrared spectroscopy to detect which types of molecules that are present in the sample. (Wilson, 2005) Molecules can also be identified by their mass using mass spectrometers, or by their molecular diffusivity using a chromatograph. One type of chromatograph is the “electrophoresis instrument”, they can be built with micro fabrication techniques and can therefore be very small. (Wilson, 2005)

Another way of identifying molecules is letting a chemical reaction take place on an electrode. In this case the electrode is the so called “exposed gate” of a field effect transistor (FET) and the electrical properties of the FET changes when the reaction takes place. The problem here is to get the device to only detect one reaction due to one specific molecule, but there are ways to coat the electrode with molecules that are very selective. (Wilson, 2005)

## **Metal oxide semiconductor, gas sensor**

Metal oxide gas sensors are mainly used for detecting changes in gas concentrations, these sensors are based on change in conductivity when in contact with the gas. The advantages of the metal oxide semiconductors are that they are highly sensitive for gases that should be detected, humidity and temperature does not affect the output to much and they are relatively cheap. (Tille, 2010)

Oxidizing gases like O<sub>2</sub> and NO<sub>2</sub> makes the metal oxide less conductive while reducing gases like CO and C<sub>x</sub>H<sub>y</sub> increase the conductivity. (Tille, 2010) The dependence of Voltage output due to CO concentration is shown below:

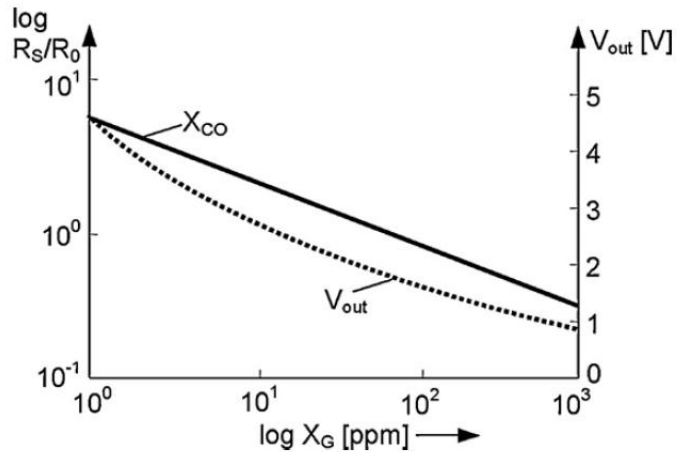


*Figure C 2.* The y-axis to the left shows the normalized output resistance,  $R_s/R_0$ , the y-axis to the right shows the output signal which is in voltages. The x-axis shows the concentration of the gas, in this case CO.

The sensor sends its signals via a control unit to an actuator, for example the fresh air flap. The flap closes when the levels of  $\text{NO}_2$  or CO are too high and as a result the cabin air is recirculated, hence minimizing the harm for the driver. Concentration limits in traffic environment for the flap to close can be 50 ppb for  $\text{NO}_2$  and 1 ppm for CO as seen in the picture below. (Tille, 2010)

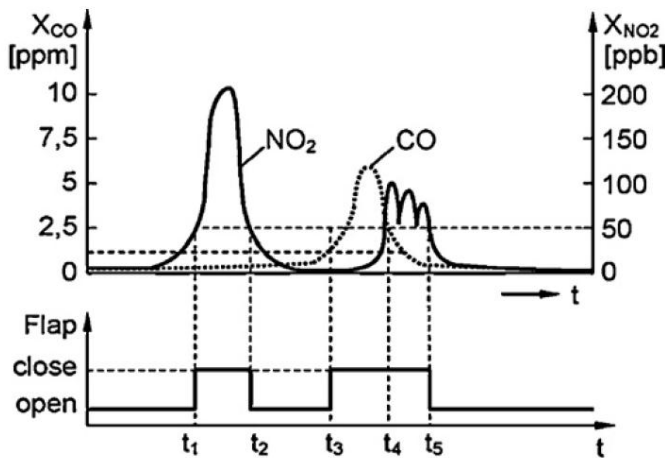


*Figure C 3.* The graph on the top show gas concentrations over time, the dotted line shows the concentration of CO, the other one the concentration of  $\text{NO}_2$ . The other graph shows when the flap is opened and closed.

As seen in the picture, the flap closes first at  $t_1$  when the concentration of  $\text{NO}_2$  is over the limit of 50 ppb, then the flap stays closed until the concentration goes down again. At time  $t_3$  there is an increase in CO and the flap closes, at time  $t_4$  the concentration of CO goes down but the concentration of  $\text{NO}_2$  goes up so the flap stays closed until  $t_5$  where the  $\text{NO}_2$  concentration is below the threshold concentration again. (Tille, 2010)

## Appendix D – Verification of the Model

A heat balance of the cabin was done by hand in order to verify that the Simulink model provides the correct output values. The heat balance was performed for a case when the outside temperature is 15 °C, the values used in the Simulink model for the same case are given in table eleven.

**Table 11.** Inputs when calculating.

$t_S$ – Temperature of incoming air [°C]	18.63
$t_{Out}$ – Temperature of outdoor air [°C]	15
$t_{Ekv}$ – Equivalent temperature [°C]	15.99
$\dot{Q}_{Sun}$ – Sun load [W/m <sup>2</sup> ]	38.077
$\dot{V}$ – Air flow [m <sup>3</sup> /s]	0.06
$\dot{Q}_{Eng}$ – Heat load from engine [W]	281.25

In the heat balance calculated by hand  $T_S$  was assumed to be unknown and the other values from table 11 was used to calculate  $t_S$ . The heat balance was calculated according to:

$$\dot{Q}_{wall,eq} + \dot{Q}_{wall} + \dot{Q}_{roof,eq} + \dot{Q}_{front,eq} + \dot{Q}_{floor} + \dot{Q}_{Window} + \dot{Q}_{HVAC} + \dot{Q}_{Engine} + \dot{Q}_{Person} = 0$$

Where the first six terms above represent the heat flux trough the sunlit walls, walls in shadow, roof, front floor and windows. The next three represent heat flux from the HVAC unit, the engine and one person. For the sides of the cabin that are sunlit an equivalent Outside Air Temperature (OAT) is used for the difference between the in cabin temperature and the actual OAT. In the equation above the sides that are sunlit are represented by the lower index *eq*, and for the sides of the cabin that are in shadow the real OAT is used. The equivalent temperature is calculated according to:

$$t_{eq}^{eq,sun} = t_o + \frac{\alpha_{Sun}}{\alpha_E} * I_{sun}$$

Where  $t_o$  is the outside temperature in °C,  $\alpha_{Sun}$  is the color dependent absorptivity factor,  $\alpha_E$  is the convection coefficient in W/(m<sup>2</sup>K) and  $I_{Sun}$  is the sun load in W/m<sup>2</sup>. (Gruber, 2012)

Each heat contribution source in the heat balance is in the equation above denoted by  $\dot{Q}$ . The heat transfer through the wall is calculated according to:

$$\dot{Q} = U * A * \Delta t$$

Where  $U$  is the overall heat transfer coefficient in W/m<sup>2</sup>K,  $A$  is the area of the wall or window in m<sup>2</sup> and  $\Delta t$  is the temperature difference between the two sides of the wall or window. (Incropera, 2007)

The heat or cooling supply from the HVAC unit is calculated according to:

$$\dot{Q}_{HVAC} = V * c_{p,air} * \rho_{air} * (t_{Cab} - t_S)$$

Where  $\dot{V}$  is the supply air flow rate in  $\text{m}^3/\text{s}$ ,  $c_{p,\text{air}}$  is the heat capacity of air in  $\text{J/kgK}$ ,  $\rho_{\text{air}}$  is the density of the air in  $\text{kg/m}^3$  and  $t_{\text{Cab}}$  is the cab air temperature in  $^{\circ}\text{C}$ .

Hence, the supply air temperature,  $t_s$ , is calculated according to:

$$t_s = t_{\text{Cab}} - \frac{(\dot{Q}_{\text{wall},eq} * \dot{Q}_{\text{wall}} * \dot{Q}_{\text{roof},eq} * \dot{Q}_{\text{front},eq} * \dot{Q}_{\text{floor}} * \dot{Q}_{\text{Engine}} * \dot{Q}_{\text{Person}})}{\dot{V} * c_{p,\text{air}} * \rho_{\text{air}}}$$

The result of  $t_s$  from the calculations above was  $18.60\ ^{\circ}\text{C}$  which can be compared with the temperature that was given by the Simulink model to be  $18.63\ ^{\circ}\text{C}$ . The calculation of the heat balance verifies the validity of the model as a difference of  $0.03\ ^{\circ}\text{C}$  between the calculation performed by hand and the results from the simulation can be considered as acceptable due to a manual tuning of the model.

## Appendix E – In Data, Simulations

**Table 12.** In data parameters used in simulations.

Input parameter	Unit	Explanation	Source / Comment
c_p_air=1000	[J/kgK]	Specific heat of air	(1)
rho_air=1.1	[kg/m3]	Density of air	(1)
h_room=1.845	[m]	Height of cabin	(2)
l_room=1.91	[m]	Length of cabin	(2)
b_room=2.1	[m]	Width of cabin	(2)
rho_plast=1200	[kg/m3]	Density of plastics	(3) (Assuming acrylic)
rho_metal=8000	[kg/m3]	Density of metal	(4)
rho_ull=190	[kg/m3]	Density of insulation material	(4)
c_p_plast=1500	[J/kgK]	Specific heat of plastics	(5)
c_p_metal=480	[J/kgK]	Specific heat of metal	(4)
c_p_ull=840	[J/kgK]	Specific heat of insulation material	(6)
m_inredning=200	[kg]	Mass of interior	(7) (This only slows down the heating, other assumptions like: all heat from the sun is directly transferred to the air in the cabin, not via interiors etc. makes this unimportant)
c_p_inredning=1500	[J/kgK]	Specific heat of interior	(7) (This only slows down the heating)
UA_window=15.20	[W/K]	UA value of windows	Calculated with lambda values from (8) and thicknesses from: (9). Lambda value for PVB from: (5)
A_window=2.26	[m2]	Total area all three windows	(2)
A_XX=xx	[m2]	Area of wall/floor/roof without the window	(change the “XX” for different walls/floor/roof) (2)
alfa_i_XX=25	[W/m2K]	Heat transfer coefficient, convection for the inside of the walls, roof and floor.	(change the “XX” for different walls/floor/roof) (10)
alfa_o_XX=10	[W/m2K]	Heat transfer coefficient, convection for the outside of the walls, roof and floor.	(change the “XX” for different walls/floor/roof) (10)
lamda_1_XX=0.25	[W/mK]	Heat transfer coefficient, conduction for plastics.	(change the “XX” for different walls/floor/roof) (5)
l_1_XX=0.003	[m]	Thickness of plastic layer.	(change the “XX” for different walls/floor/roof) (2)
lamda_2_XX=0.037	[W/mK]	Heat transfer coefficient, conduction for insulation material.	(change the “XX” for different walls/floor/roof) (11)
l_2_XX=*	[m]	Thickness of insulation material	(change the “XX” for different walls/floor/roof)

		layer.	(2) (*0.03 for walls 0.02 for roof/floor)
lamda_3_XX=17	[W/mK]	Heat transfer coefficient, conduction for metal.	(change the "XX" for different walls/floor/roof) (11)
L_3_XX=0.001	[m]	Thickness of metal layer.	(change the "XX" for different walls/floor/roof) (2)
R_X_XX=xx	[%]	A percentage, how much of the heat from a source is in form of radiation.	(1) For sun light: all heat is assumed to go directly to the air, not via interiors. This is done to "fasten up" the heating to get an extreme case.

The following parameters were changed for each simulated case.

**Table 13.** In data parameters used in simulations.

Input parameter name	Unit	Explanation	Comment
ts	[°C]	Temperature on the air coming in to the cabin from the HVAC module.	Was tuned in for each supply air flow rate
pers	[#]	Number of persons in the cabin.	One person in all simulations.
to	[°C]	Compensated outside temperature.	To compensate for that a surface gets hotter when sunlit.
Sun Load	[W]	Sun load	Different sun loads were tested.
Supply Air Flow Rate	[m <sup>3</sup> /s]	Air flow from HVAC module via the fan.	40 l/s to 70 l/s was tested.
Engine	[W]	Extra heat from engine.	See how it's calculated above.
Floor	[W]	Heat "supposed" to go out through the floor. Have to be added to compensate for since the model use the same values for floor and roof.	Assumption: no heat is leaking out through the floor.
Start value	[°C]	Initial wall and air temperature inside the cabin.	21 °C for all simulations.

### In data sources:

- (1) Standard values built in, inside the model.
- (2) Measured approximately in existing Volvo truck.
- (3) DOTMAR engineering plastic products, plastic properties Tables, Accessed: 4 may 2012.  
<http://www.dotmar.com.au/density.html>
- (4) Fundamentals of Heat and Mass Transfer; Incropera, DeWitt, Bergman, Lavine; John Wiley & Sons, Inc; 2007; USA; 6th edition.
- (5) Professional Plastics, Thermal Properties of Plastic Materials, Accessed: 4 may 2012.  
<http://www.professionalplastics.com/professionalplastics/ThermalPropertiesofPlasticMaterials.pdf>
- (6) The Engineering ToolBox, solids – Specific Heats, Accessed: 4 may 2012.  
[http://www.engineeringtoolbox.com/specific-heat-solids-d\\_154.html](http://www.engineeringtoolbox.com/specific-heat-solids-d_154.html)
- (7) Guessed, not important.
- (8) VVS Tabeller och diagarm, VVS-Tekniska Föreningen och Förlags AB VVS, Förlags AB VVS, Stockholm 1974
- (9) Volvo GTT, Internal document 4.
- (10) Värmeöverföring, strömningssystem och fuktig luft, kursmaterial Sektionen för Väg- och vattenbyggnad, Installationsteknik, chalmers tekniska högskola, Göteborg 2003.
- (11) Jernkontorets energihandbok, Byggnader, Tabell-Värmeledning och U-värden för olika material. 2008-05-16, Accessed: 4 may 2012.  
<http://energihandbok.se/x/a/i/10673/Tabell---Varmeledningsformaga-och-U-varden-for-olika-material.html>

## Appendix F – Cooling Potential

As seen in the result from the simulation, a bigger air flow can handle bigger sun loads, there is a “bigger cooling potential” with a bigger air flow. This is easiest explained with an example: The cooling load demand is calculated by:

$$\dot{Q}_{cool} = \dot{V} * c_p * \rho * (t_{cabin} - t_s)$$

Where  $\dot{V}$  is the supply air flow rate,  $c_p$  and  $\rho$  is the specific heat and density for air and can be approximated to be constant for small temperature changes.  $t_{cabin}$  is the temperature in the cabin and  $t_s$  is the temperature of the air supplied by the HVAC module into the cabin (the supply air temperature). In the two cases below different supply air flow rates are chosen and the temperature into the cabin is tuned so that the temperature in the cabin is kept constant.

**Case 1;**  $\dot{V} = 1$ ,  $t_s$  is tuned in to keep the temperature inside the cabin,  $t_{cabin}$ , at 2 °C,  $t_s$  became 1 °C. Now the temperature in the cabin is kept constant at 2 °C, and the cooling load is equal to  $c_p$  times  $\rho$ .

$$\dot{Q}_{cool} = 1 * c_p * \rho * (2 - 1) = c_p * \rho$$

After the sun load is applied the temperature in the cabin is 3 °C.

$$\dot{Q}_{cool} = 1 * c_p * \rho * (3 - 1) = c_p * \rho * 2$$

As seen above the cooling load has doubled without having to increase air flow or lower the supply air temperature.

**Case 2;**  $\dot{V} = 2$ ,  $t_s$  is tuned in to keep the temperature inside the cabin,  $t_{cabin}$ , at 2 °C,  $t_s$  became 1.5 °C. Now the temperature in the cabin is kept constant at 2 °C, and the cooling load is equal to  $c_p$  times  $\rho$ .

$$\dot{Q}_{cool} = 2 * c_p * \rho * (2 - 1.5) = c_p * \rho$$

As seen, to maintain the temperature of 2 °C in the cabin the same cooling load is applied as in case 1, the difference is that a bigger “part” of the cooling load is in this case from the supply air flow.

Now the temperature in the cabin has increased to 3 °C due to the sun load:

$$\dot{Q}_{cool} = 2 * c_p * \rho * (3 - 1.5) = c_p * \rho * 3$$

As seen above in this case the cooling load is tripled. Hence there is a “bigger cooling potential” with a bigger air flow.



## Appendix G – Outside Sun Load

The step of solar heat gain used in the simulations was the sun load entering the cabin. The solar radiation outside the vehicle and the solar heat gain are related according to the equation below.

*Outside sun load*

$$= (\text{Entering Sun Load}) / (\text{Window area hit by the sun} * \text{Transmission factor of the windows})$$

The windows have different transmission factors, so for the case when the sun hits both a side window and the windshield the transmission factors were weighted due to their part of the area. (The transmissions factors are found in Volvo GTT, Internal document 4)

First the biggest possible area was used, to get the worst case scenario.

**Table 14.** Transmission factors and projected area of the windows.

	Transmission factor	Part of total window area	Weighted transmission factor	Total area [m <sup>2</sup> ]
Windshield	89%	88%	87%	1.386
Side window	76%	12%		

The case where the sun hits directly on the front of the truck.

**Table 15.** Transmission factor and area of the windshield.

	transmission factor	total area [m <sup>2</sup> ]
Windshield	89%	1.3

What the solar sensor measures (assuming the control system compensates for the projected area of the sun) was calculated like this:

$$\text{Measured Sun Load } \left[ \frac{W}{m^2} \right] = \text{Entering Sun Load } [W] / \text{Window Area Hit by the Sun } [m^2]$$



## Appendix H – Benchmark of AQS and Fog Sensor

### Fog Sensor

The manufacturers of fog sensors contacted are presented in table one.

Manufacturer	Response
Casco	Did not Provide Data Sheets
E+E Elektronik	Did not Deliver Complete Solutions
GE Measurement & Control	Did Provide Information Sheets
Honeywell	Did have Fog Sensor Suitable for Vehicles
Measurement Specialties	Did not Provide Data Sheets
Sensata Technologies	Did Provide Data Sheets
Sensirion	Did not Provide Data Sheets

The content of the data sheets provided by the manufacturers that did want to participate in the benchmark are presented in table two.

	GE - Integrated Dew Point and Glass Temperature (1)	GE - Integrated Dew Point and Glass Temperature (2)	Sensata – Relative Humidity and Temperature Sensor
Humidity Range [% RH]	0 to 95	---	0 to 98
Response Time [s]	10 to 20	10 to 20	Humidity < 10 Temperature < 30
Accuracy	Dew Point $\pm$ 1.5 °C (at 25 °C and 50 % to 90 % RH) Glass Temp $\pm$ 0.6 °C (at - 10 °C to 50 °C)	Humidity $\pm$ 4.5 % RH (at 20 % to 80 % RH) Ambient Temp. $\pm$ 0.5 °C (at 25 °C) Glass Temp $\pm$ 0.3 °C (at 25 °C)	Humidity $\pm$ 4.0 % RH (Initial accuracy at - 5°C to + 30 °C) Temperature $\pm$ 0.5 °C
Operating Temperature [°C]	- 40 °C to + 120 °C	- 40 °C to + 105 °C	- 40 °C to 85 °C
Storage Temperature [°C]	---	---	- 40 °C to 85 °C
Operating Voltage Range	5 $\pm$ 0.5 [DCV]	5 $\pm$ 0.5 [VDC]	5 $\pm$ 0.25 [V]
Output Voltage [V]	0 to 4.1	---	0 to 5
PIN Assignment [-]	---	---	MQS – 3 pin – code 8
Power Consumption	< 5 [mW]	< 5 [mW] (at 5 DCV and 25 °C)	10 [mA]
Size [mm]	---	---	42.8 * 31.3 * 29.3
Weight [g]	---	---	< 20
Package Material [-]	Polyamide 6/6	---	PA
Output Type [-]	---	Analog + Digital (2-wire)	Open Collector PWM or LIN 2.0
Environmental Protection [-]	---	---	IP 64 + IP 67

## AQS Sensor

The manufacturers of AQS contacted are presented in table three.

Manufacturers	Response
AppliedSensor	Supplied Data Sheets
Behr Group	Did not Provide Data Sheets
City Technology	Did not Provide Data Sheets
GE Measurement & Control	Supplied Data Sheets
FIGARO	Not Suitable for Vehicles
Hanwei	No Complete Solution
Honeywell	Not Suitable for Vehicles
KWJ Engineering	No Complete Solution
Paragon	Did not Provide Data Sheets
Red-ant	Did not Provide Data Sheets
Sensata Technologies	Supplied Data Sheets
Siemens	Not Suitable for Vehicles
Sierra Monitor Corp.	Not Suitable for Vehicles

The content of the data sheets provided by the manufacturers that did want to participate in the benchmark are presented in table two.

	Sensata Technologies – Air Classification Module	AppliedSensor – Air Quality Sensor	GE Measurement & Control – Air Quality Sensor
Detectable Gases	CO, NO <sub>2</sub> and HC	CO, NO <sub>2</sub> and VOC	NO <sub>x</sub> , SO <sub>x</sub> , CO, LPG and CH <sub>x</sub>
Concentration Range	CO: 0 to 200 [PPM] NO <sub>2</sub> : 0 to 2 [PPM]	CO/VOC: 0 to 200 [PPM] NO <sub>2</sub> : 0 to 2 [PPM]	CO/LPG/CH <sub>x</sub> : 2 to 18 [PPM] NO <sub>x</sub> /SO <sub>x</sub> : 100 to 900 [PPB]
Limit of Detection	CO: 2 [PPM] NO <sub>2</sub> : 2 [PPB]	---	---
Response Time	CO: 1 [s] NO <sub>2</sub> : 2 [s]	---	---
Maximum Humidity	---	---	95 [% RH]
Operating Temperature	- 40 to + 85 [°C]	---	- 30 to + 80 [°C]
Storage Temperature	- 40 to + 85 [°C]	---	---
Air Velocity Range	0.5 to 10 [m/s]	---	---
Operating Voltage Range	9 to 16.5 [VDC]	12 [V]	9 to 16 [VDC]
Output Voltage [V]	---	---	0 to 5 [V]
PIN Assignment [-]	MQS - 3 pin - code 8	---	---
Power Consumption	< 1 [W]	550 mW	---
Maximum Current Rate	---	---	3/300 [mA]
Size	42.8 * 31.3 * 29.3 [mm]	56 * 29 * 14 [mm]	---
Weight	< 20 [g]	10 [g]	---
Package Material	PA	---	---
Output type	Open Collector PWM or LIN 2.0	PWM, LIN	---
Environmental Protection	P 64 + IP67	---	---

## Appendix I – Equations Used in Simulink Model

Below the final form of the equations used to model building and HVAC-components are presented. For each model, the input, output and model parameters are presented. The parameters have either been treated as varying from one model to another or as constant throughout the study. First, the constant reappearing model parameters are presented.

Reappearing constant model parameters:  $c_{p,a}$  (specific heat capacity of air, 1000 J/(kg.K)),  $c_{p,i}$  (specific heat capacity of air, 1200 J/(kg.K)),  $\rho_a$  (density of air),  $\rho_w$  (density of water),  $c_{p,w}$  (specific heat capacity of water),

### Room model: thermal and CO<sub>2</sub> concentration

Input variables:  $\dot{V}_s$  (supply air flow rate),  $t_s$  (temperature of supply air),  $c_s$  (CO<sub>2</sub> concentration of the supply air),  $\dot{Q}_{FCU,heat}$  (heat supply rate),  $\dot{Q}_{FCU,cooling}$  (heat extraction rate)

Output variables:  $t_r$  (room air temperature),  $c_r$  (room air CO<sub>2</sub> concentration),  $t_{surf,ie}$  (surface temperature of interior building elements, i.e. walls, floor and roof),  $t_{surf,ow}$  (surface temperature of exterior wall)

Disturbances:  $t_{adj}$  (air temperature of adjacent rooms),  $t_o$  (outdoor air temperature),  $\dot{V}_{door}$  (air flow rate through door),  $\dot{V}_{inf}$  (infiltration flow rate),  $\dot{Q}_{light}$  (heat emitted by lighting),  $n_{people}$  (number of people),  $\dot{Q}_{equip}$  (heat emitted by equipment),  $\dot{Q}_{sun}$  (solar heat gain)

Variable model parameters:  $V_r$  (room volume),  $m_i$  (mass of interior),  $U_{win}$  (overall heat transfer coefficient of window),  $A$  (area of building element),  $\dot{q}_{people}$  (specific heat emitted by people),  $c_{p,ie}$  (specific heat capacity of internal building element),  $\rho_{ie}$  (density of internal building element),  $\rho_{ow}$  (density of exterior wall),  $c_{p,ow}$  (specific heat capacity of exterior wall),  $V_{ie}$  (thermally active volume of interior building element),  $V_{ow}$  (thermally active volume of exterior wall),  $U'_{ie}$  (convective and conductive heat transfer coefficient of interior building element),  $U'_{ow}$  (convective and conductive heat transfer coefficient of exterior wall)

Constant model parameters:  $\alpha_i$  (room-side convective heat transfer coefficient, 6.9 W/(m<sup>2</sup>.K)),  $\alpha_{adj}$  (convective heat transfer coefficient of adjacent room 6.9 W/(m<sup>2</sup>.K)),  $\alpha_o$  (convective heat transfer coefficient of external wall 6.9 W/(m<sup>2</sup>.K)),  $R_{conv}$  (part of heat transferred by convection, values presented in table 4.1),  $c_{p,i}$  (specific heat capacity of interior, 1255 J/(kg.K)),



$$\begin{aligned}
\frac{dt_r}{d\tau} \cdot (V_r \cdot \rho_a \cdot c_{p,a} + m_i \cdot c_{p,i}) &= \dot{V}_s \cdot \rho_a \cdot c_{p,a} \cdot (t_s - t_r) \\
&+ \dot{V}_{inf} \cdot \rho_a \cdot c_{p,a} \cdot (t_0 - t_r) + \dot{V}_{door} \cdot \rho_a \cdot c_{p,a} \cdot (t_{adj} - t_r) \\
&+ U_{win} \cdot A_{win} \cdot (t_0 - t_r) + \alpha_i \cdot A_{ow} \cdot (t_{surf,ow} - t_r) \\
&+ \sum_{n=1}^4 \alpha_{i,n} \cdot A_{surf,ie,n} \cdot (t_{surf,ie,n} - t_r) + R_{conv,sun} \cdot \dot{Q}_{sun} \\
&+ n_{people} \cdot R_{conv,people} \cdot \dot{q}_{people} + R_{conv,equip} \cdot \dot{Q}_{equip} \\
&+ R_{conv,light} \cdot \dot{Q}_{light} + R_{conv,FCU} \cdot \dot{Q}_{FCU,heat} + R_{cr,FCU} \cdot \dot{Q}_{FCU,cooling}
\end{aligned}$$

$$\begin{aligned}
\frac{dt_{surf,ie,1}}{d\tau} \cdot (V_{ie,1} \cdot \rho_{ie,1} \cdot c_{p,ie,1}) &= A_{ie,1} \cdot U'_{ie,1} \cdot (t_{surf,ie,1} - t_{adj,1}) \\
&+ \alpha_i \cdot A_{surf,ie,1} \cdot (t_r - t_{surf,ie,1}) + \frac{1}{R_{conv,sun,ie,1}} \cdot \dot{Q}_{sun} \\
&+ n_{people} \cdot \frac{1}{R_{conv,people,ie,1}} \cdot \dot{q}_{people} + \frac{1}{R_{conv,equip,ie,1}} \cdot \dot{Q}_{equip} \\
&+ \frac{1}{R_{conv,light,ie,1}} \cdot \dot{Q}_{light} + \frac{1}{R_{conv,FCU,ie,1}} \cdot \dot{Q}_{FCU,heat} \\
&+ \frac{1}{R_{cr,FCU,ie,1}} \cdot \dot{Q}_{FCU,cooling}
\end{aligned}$$

⋮

$$\begin{aligned}
\frac{dt_{surf,ie,4}}{d\tau} \cdot (V_{ie,4} \cdot \rho_{ie,4} \cdot c_{p,ie,4}) &= A_{ie,4} \cdot U'_{ie,4} \cdot (t_{surf,ie,4} - t_{adj,4}) \\
&+ \alpha_i \cdot A_{surf,ie,4} \cdot (t_r - t_{surf,ie,4}) + \frac{1}{R_{conv,sun,ie,4}} \cdot \dot{Q}_{sun} \\
&+ n_{people} \cdot \frac{1}{R_{conv,people,ie,4}} \cdot \dot{q}_{people} + \frac{1}{R_{conv,equip,ie,4}} \cdot \dot{Q}_{equip} \\
&+ \frac{1}{R_{conv,light,ie,4}} \cdot \dot{Q}_{light} + \frac{1}{R_{conv,FCU,ie,4}} \cdot \dot{Q}_{FCU,heat} \\
&+ \frac{1}{R_{cr,FCU,ie,4}} \cdot \dot{Q}_{FCU,cooling}
\end{aligned}$$

$$\begin{aligned}
\frac{dt_{surf,ow}}{d\tau} \cdot (V_{ow} \cdot \rho_{ow} \cdot c_{p,ow}) &= A_{ow} \cdot U'_{ow} \cdot (t_{surf,ow} - t_o) \\
&+ \alpha_i \cdot A_{surf,ow} \cdot (t_r - t_{surf,ow}) + \frac{1}{R_{conv,sun,ow}} \cdot \dot{Q}_{sun} \\
&+ n_{people} \cdot \frac{1}{R_{conv,people,ow}} \cdot \dot{q}_{people} + \frac{1}{R_{conv,equip,ow}} \cdot \dot{Q}_{equip} \\
&+ \frac{1}{R_{conv,light,ow}} \cdot \dot{Q}_{light} + \frac{1}{R_{conv,FCU,ow}} \cdot \dot{Q}_{FCU,heat} \\
&+ \frac{1}{R_{cr,FCU,ow}} \cdot \dot{Q}_{FCU,cooling}
\end{aligned}$$

$$\begin{aligned}
\frac{dc_r}{d\tau} \cdot (V_r) &= \dot{V}_s \cdot (c_s - c_r) + \dot{V}_{inf} \cdot (c_o - c_r) + \dot{V}_{door} \cdot (c_{adj} - c_r) \\
&+ n_{people} \cdot \dot{m}_{CO_2}
\end{aligned}$$

where

$$U'_{ie} = \frac{1}{\frac{I}{\alpha_{adj}} + \sum \frac{d_{ie}}{\lambda_{ie}}} \quad U'_{ow} = \frac{1}{\frac{I}{\alpha_o} + \sum \frac{d_{ow}}{\lambda_{ow}}}$$

### Flow rate through door

Input variables:  $h_{door}$  (door opening),  $t_{adj}$  (adjacent room temperature),  $t_r$  (room temperature)

Output variables:  $\dot{V}_{door}$  (flow rate through door)

Model parameters:  $A_{door}$  (area of door),  $H_{door}$  (height of door)

$$\dot{V}_{door} = 0.03 \cdot h_{door} \cdot A_{door} \cdot \left( H_{door} \cdot |t_{adj} - t_r| \right)^{0.5}$$

